
Science
Translational
Medicine
STM collections
STM collections
STM collections
STM collections
STM collections
STM collections
STM collections
STM collections
STM collections
STM collections
STM collections
STM collections
STM collections
STM collections
STM collections
STM collections
Online issue 19 December 2012

Science Translational Medicine
AAAS

Long-Term Follow-Up After Gene Therapy for Canavan Disease

Paola Leone *et al.*

Sci Transl Med **4**, 165ra163 (2012);
DOI: 10.1126/scitranslmed.3003454

Editor's Summary

Gene Therapy for Canavan Disease

Canavan disease is a fatal childhood neurodegenerative disorder for which there is no effective treatment. It is caused by a defect in a single gene (*ASPA*) that results in a deleterious buildup of *N*-acetyl-aspartate in the brain. This process starts at birth and is accompanied by a failure to form and maintain myelin, the protective sheath surrounding nerves. As a brain-specific disorder with simple Mendelian inheritance, Canavan disease represents an excellent target for enzyme replacement using gene therapy. Leone *et al.* now report the long-term results of gene therapy in 13 Canavan disease patients using adeno-associated viral vector delivery of the *ASPA* gene. The investigators found that gene therapy was safe and led to a decrease in *N*-acetyl-aspartate in the brain, together with decreased seizure frequency and clinical stabilization. Clinical stabilization was greatest in the youngest patients. Early detection and treatment with gene therapy–mediated enzyme replacement in the neonatal period may offer the best opportunity for a reduction in symptoms and long-term stabilization in patients with Canavan disease.

Science Translational Medicine (print ISSN 1946-6234; online ISSN 1946-6242) is published weekly, except the last week in December, by the American Association for the Advancement of Science, 1200 New York Avenue NW, Washington, DC 20005.

GENE THERAPY

Long-Term Follow-Up After Gene Therapy for Canavan Disease

Paola Leone,[1]* David Shera,[2] Scott W.J. McPhee,[3] Jeremy S. Francis,[1] Edwin H. Kolodny,[4] Larissa T. Bilaniuk,[5] Dah-Jyuu Wang,[5] Mitra Assadi,[6] Olga Goldfarb,[6] H. Warren Goldman,[6] Andrew Freese,[7] Deborah Young,[8] Matthew J. During,[8,9] R. Jude Samulski,[3,10] Christopher G. Janson[7,11]

Canavan disease is a hereditary leukodystrophy caused by mutations in the aspartoacylase gene (*ASPA*), leading to loss of enzyme activity and increased concentrations of the substrate *N*-acetyl-aspartate (NAA) in the brain. Accumulation of NAA results in spongiform degeneration of white matter and severe impairment of psychomotor development. The goal of this prospective cohort study was to assess long-term safety and preliminary efficacy measures after gene therapy with an adeno-associated viral vector carrying the *ASPA* gene (AAV2-*ASPA*). Using noninvasive magnetic resonance imaging and standardized clinical rating scales, we observed Canavan disease in 28 patients, with a subset of 13 patients being treated with AAV2-*ASPA*. Each patient received 9×10^{11} vector genomes via intraparenchymal delivery at six brain infusion sites. Safety data collected over a minimum 5-year follow-up period showed a lack of long-term adverse events related to the AAV2 vector. Posttreatment effects were analyzed using a generalized linear mixed model, which showed changes in predefined surrogate markers of disease progression and clinical assessment subscores. AAV2-*ASPA* gene therapy resulted in a decrease in elevated NAA in the brain and slowed progression of brain atrophy, with some improvement in seizure frequency and with stabilization of overall clinical status.

INTRODUCTION

Canavan disease is a rare autosomal recessive leukodystrophy caused by mutations in the *ASPA* gene encoding aspartoacylase (*1*–*3*), a zinc carboxypeptidase enzyme (*4*) that deacetylates *N*-acetyl-aspartate (NAA). Normally, aspartoacylase is found in oligodendrocyte progenitor (O2A) cells and oligodendrocytes in the brain (*5*–*8*), with smaller amounts in microglia and brainstem neurons (*9*). Outside of the brain, aspartoacylase is present in peripheral tissues such as skin and kidney (*3*), but its only known role is the degradation of NAA in the brain. Deficiency of aspartoacylase in Canavan disease leads to a linear increase in brain NAA concentrations over time, with whole-brain concentrations rising to 8 to 14 mM compared to a normal range of 3 to 8 mM (*10*). This is despite a compensatory decrease in the rate of NAA synthesis through down-regulation of NAA synthase (*11*). NAA, one of the most prevalent small molecules in the brain, comprises more than 0.1% of the brain by weight (*12*, *13*) and is involved in brain development and homeostasis (*14*). NAA appears to be synthesized exclusively in neurons and has been isolated from mitochondrial and microsomal fractions (*15*–*18*). It is found throughout the neuronal cytoplasm, dendrites, and axons (*19*, *20*), where it normally forms a steep concentration gradient with respect to the extracellular space (*21*, *22*). NAA and a related dipeptide *N*-acetyl-aspartyl-glutamate (NAAG) are transported from the cytoplasm to the extracellular space by an unidentified transporter, and NAA is taken up by glia through a dicarboxylic acid transporter (*23*) before hydrolysis by aspartoacylase. In addition to high concentrations normally found within neurons, NAA is detected at lower concentrations in oligodendrocytes (*24*) during induction of ASPA expression during early postnatal development (*25*, *26*). Evidence to date suggests that the pathological effects of globally elevated NAA in Canavan disease are multifactorial and are related to its diverse physiological roles as an organic osmolyte (*21*, *27*), water cotransporter in metabolically active cells (*28*), myelin precursor (*7*, *25*, *29*–*33*), intermediate for NAAG (*34*, *35*), and putative signal molecule in the development and migration of oligodendrocytes (*26*).

The pathology of Canavan disease is most evident in subcortical white matter where high concentrations of NAA in the interstitial space have complex effects. Canavan disease is associated with aberrant myelination, brain edema, and gross morphological changes in major white matter tracts, with clinical sequelae that include macrocephaly, severe cognitive and motor delay, epilepsy, and death typically by the third decade. The essential pathological feature of Canavan disease is dysmyelination with intramyelinic edema and extensive central white matter vacuolation. Ultrastructural studies report splitting of myelin lamellae along the intraperiod line (*36*–*38*), similar to the effects seen in certain types of direct chemical attack on the myelin sheath (*39*). These effects probably result from biosynthetic defects in myelin (*33*) in conjunction with localized periaxonal osmotic effects due to increased NAA. Other reported abnormalities include misshapen mitochondria in swollen astrocytes (*40*), suggesting a metabolic imbalance. Although classical postmortem studies have shown limited pathology in neurons (*38*), the prevalence of epilepsy implies abnormal membrane depolarization (*41*, *42*). The early literature proposed three clinical variants of

[1]Department of Cell Biology, Cell & Gene Therapy Center, University of Medicine & Dentistry of New Jersey, Stratford, NJ 08034, USA. [2]Division of Biostatistics, Children's Hospital of Philadelphia, Philadelphia, PA 19104, USA. [3]Asklepios Biopharmaceuticals, Chapel Hill, NC 27517, USA. [4]Department of Neurology, New York University School of Medicine, New York, NY 10016, USA. [5]Division of Neuroradiology, Children's Hospital of Philadelphia, Philadelphia, PA 19104, USA. [6]Cooper Neurological Institute, Camden, NJ 08103, USA. [7]Department of Neurosurgery, University of Minnesota Medical School, Minneapolis, MN 55455, USA. [8]Departments of Molecular Medicine and Pathology, and Clinical Pharmacology, University of Auckland, Auckland 1023, New Zealand. [9]Departments of Neuroscience and Molecular Virology, Immunology & Medical Genetics, Ohio State University, Columbus, OH 43210, USA. [10]Department of Pharmacology, Gene Therapy Center, University of North Carolina, Chapel Hill, NC 27599, USA. [11]Department of Neurology, University of Minnesota Medical School, Minneapolis, MN 55455, USA.
*To whom correspondence should be addressed. E-mail: leonepa@umdnj.edu

Canavan disease with a usual prognosis of death before adolescence. However, this classification is now viewed as flawed (*43*) with recommendations to use a gene-based diagnosis of typical versus mild Canavan disease instead. Most *ASPA* mutations in Canavan disease are functionally equivalent (*44*) with nearly total loss of enzyme activity, and patients with typical mutations are uniformly severely affected. Although the natural history of Canavan disease involves increased whole-brain NAA concentrations (*10*) and progressive disability, prolonged survival to adulthood has been reported as a result of better supportive care (*45*) including treatment with antiepileptics and other medications (*46*), as well as gastric feeding tubes, orthotics, and physical therapy. Hence, for patients with typical Canavan disease, long-term survival reflects specific effects of drugs or other therapies, as well as improvements in general medical care rather than genetic variability.

The rationale for using adeno-associated viral vector gene therapy (AAV2-*ASPA*) for treating Canavan disease was based, in part, on our previous experience with *ASPA* human gene therapy using a nonviral vector [LPD (liposome-encapsulated, condensed plasmid DNA)–*ASPA*] in 14 patients in 1999, which had suggested a partial reversal of elevated NAA concentrations (*46*, *47*). The development of neurotropic viral vectors with superior gene expression capabilities and a favorable safety profile led to approval in 2001 by the National Institutes of Health (NIH) Recombinant DNA Advisory Committee for a gene therapy clinical protocol for Canavan disease using recombinant AAV2 (*48*). Concurrent studies of native human aspartoacylase in an *ASPA* knockout mouse model (*49*) and the *ASPA* null rat (*50*) suggested that brain NAA concentrations decrease after treatment with AAV2-*ASPA*, resulting in behavioral and histopathological improvements, including a decline in seizure frequency. The current phase 1/2 clinical trial with AAV2-*ASPA* gene therapy was designed to assess long-term safety and to establish dosing parameters. Safety was determined by analysis of adverse events and trends in clinical assessments. A secondary goal was to assess efficacy, defined as a decrease in pathologically elevated NAA concentrations together with favorable trends in secondary outcomes. NAA was selected as the primary outcome measure for disease progression because abnormally elevated NAA is the biological hallmark of Canavan disease and may be measured quantitatively in the brain using noninvasive proton magnetic resonance spectroscopy (^{1}H-MRS) (*10*).

RESULTS

Patient recruitment and study protocol

Subjects were recruited internationally with the participation of nonprofit research foundations. Institutional review board approvals were obtained at all participating sites. Twenty-eight subjects were enrolled from the United States, Brazil, England, Germany, Italy, and Venezuela, from which a cohort of 13 subjects received treatment with AAV2-*ASPA*. Inclusion criteria were a definitive diagnosis of Canavan disease with at least one positively identified gene mutation and ages between 3 and 96 months (Table 1). All prospective subjects underwent genotyping. After skin biopsy, each patient's *ASPA* mutation was determined and fibroblasts were analyzed for aspartoacylase activity (*51*), which, in all cases, showed absence of enzyme activity (<4% wild type). Recently, a unique mutation that confers an unusually benign phenotype was discovered (*52*), but this rare variant was not included. Subjects were assigned to gene therapy or monitoring with the oldest patients treated first according to U.S. Food and Drug Administration (FDA) recommendations to optimize the risk-benefit ratio. Three groups of subjects were treated in 2001, 2003, and 2005, which corresponded to separate AAV2-*ASPA* production runs. Treatment groups were generally equivalent in phenotype, but the oldest subjects were treated first. The mean

Table 1. Demographics of treated Canavan disease patients. Subjects are presented in their order of treatment from 2001 to 2005, with their initial age (in months) at the time of gene therapy. The sequential treatment groups are divided by double lines, each corresponding to a separate lot of AAV-*ASPA*. The treatment groups were sequentially stratified by age (that is, oldest, mixed age, and youngest) but were homogeneous in phenotype. For ease of comparison, pretreatment seizure history is graded into three categories: –, no documented seizures; +, at least one generalized seizure (absence, myoclonic, or tonic-clonic) in the past 36 months; ++, clinically evident absence-like seizures at least monthly, or greater than three myoclonic or tonic-clonic seizures in the preceding 12 months.

Subject ID	Sex	Age	ASPA mutations	Gene therapy	Baseline seizures
01-118-04	F	83	854A→C (E285A)693C→A (Y231X)	2001	+
01-118-09	M	45	854A→C (E285A)854A→C (E285A)	2001	+
01-118-07	M	65	854A→C (E285A)854A→C (E285A)	2001	+
01-118-12	F	22	859G→A (A287T) frameshift 10T→G; 11insG	2003	–
01-118-08	F	24	Splicing IVS1-2 A→T deletion	2003	–
01-118-02	F	56	854A→C (E285A)854A→C (E285A)	2003	++
01-118-15	F	36	640G→T (E214X)914C→A (A305E)	2003	++
01-118-01	M	47	914C→A (A305E)914C→A (A305E)	2003	+
01-118-05	M	59	914C→A (A305E)548C→A (P183H)	2003	++
01-118-03	F	53	854A→C (E285A)854A→C (E285A)	2003	+
01-118-33	F	4	914C→A (A305E) deletion	2005	–
01-118-27	F	21	854A→C (E285A)854A→C (E285A)	2005	+
01-118-24	M	23	548 C→A (P183H) deletion	2005	–

ages at the time of gene therapy were 64, 42, and 16 months for the respective treatment groups. Subjects who met enrollment criteria but who were not initially assigned to a treatment group underwent magnetic resonance imaging (MRI) and clinical assessments as part of a parallel study. Clinical monitoring guidelines were established (*48*) to ensure that clinically significant deviations in laboratory values, cognitive function, or motor function would be brought to the attention of study investigators. The clinical trial study design, including patient recruitment, clinical monitoring, and outcome measures (that is, NAA spectroscopy, brain atrophy measurements, and clinical assessments) have been described (*10*, *48*, *53*).

NAA brain concentrations in Canavan disease patients after gene therapy

NAA concentrations were measured longitudinally in all subjects in four representative brain regions using single-voxel ^{1}H-MRS. In parallel with the administration of gene therapy in 13 human subjects, noninvasive measurements of NAA were obtained in an overlapping set of 28 subjects (*10*). Because NAA concentrations may not directly reflect myelination or other clinically relevant changes, secondary outcomes were also included in the analysis. The protocol required a minimum of 12 months of follow-up for the primary outcome measure of NAA data collection, but funding was available for 48 months of ^{1}H-MRS imaging for all treated subjects and for 60 months of standardized clinical assessments. Two subjects (01-118-03 and 01-118-12) were lost to long-term safety follow-up 6 years after treatment due to voluntary withdrawal on the part of the parents, but the primary endpoints had been reached.

Previous studies have shown that whole-brain NAA concentrations rise linearly in untreated Canavan disease subjects, peaking at 12 to 14 mM with an increasing rostral-caudal gradient (*47*). This pattern is also evident in our data, with the mean occipital concentrations of NAA being 2 mM higher than frontal concentrations at baseline (Fig. 1). Untreated subjects showed a monotonic increase in NAA with positive slopes in all regions except for the basal ganglia, which had a flat or slightly negative slope but remained grossly elevated at more than twice the normal concentration. After AAV-*ASPA* gene therapy, we found a reversal in pathological whole-brain NAA accumulation (Fig. 1). The analysis is based on data from 13 treated Canavan disease subjects (Table 1) as well as data from 15 untreated Canavan disease subjects (*10*, *48*) (table S1). For each of the 13 treated subjects, the mean number of pretreatment observations per brain region was 3.5 (range, 2 to 6), and the mean number of posttreatment observations per individual brain region was 5.3 (range, 2 to 11). The total number of patient-region-visits for the 28 subjects altogether was 262 before gene therapy and 274 after gene therapy.

Pretreatment NAA concentrations were modeled using both pretreatment and posttreatment data, which provide a more precise assessment of pretreatment trends. This approach showed small differences from previous estimates computed using only pretreatment data, the main difference being that pretreatment fitted slopes were increasing, whereas posttreatment slopes were decreasing. Data were fit with a longitudinal, mixed-effect generalized linear model (*54*) with subject-specific coefficients for intercept, pretreatment slope, and posttreatment slope. Covariates in the list of fixed effects included time, indicators of immediate posttreatment and 3 months posttreatment to account for effects of surgery, indicators of region, and interactions of other covariates with region. At least one subject received lithium for a brief period before gene therapy (*55*), which was taken into account in the covariates. Three of the oldest subjects in the first treatment group had received nonviral gene therapy more than 3 years before initiation of AAV2-*ASPA* gene therapy, but long-term effects were believed to be negligible and patients were considered to be naïve to treatment with AAV2-*ASPA*. This was prospectively stated in our clinical protocol as part of inclusion/exclusion criteria (*48*).

After gene therapy, we detected statistically significant changes in NAA concentrations in several brain regions (Table 2), with maximal effects in the periventricular and frontal regions. This apparent treatment effect was consistent across all regions, with 11 of 13 subjects showing a negative posttreatment slope in the frontal region and 13 of 13 showing a negative posttreatment slope in the periventricular, occipital, and basal ganglia regions (fig. S1). Although unexpected, the transient rise in NAA observed at the time of initial administration of AAV2-*ASPA* was consistent with solute flux during brain osmoregulation and was fit using a ramp function. Inferences regarding changes in NAA concentrations were tested using the Wald statistic for posttreatment slope versus zero and the change from before treatment to after treatment (*54*). In addition to fitting data from all brain regions, we performed separate model fitting for data from each region to examine the robustness of the results. Because the first treatment group was older, we also considered the possibility that the observed decline in NAA concentrations was due to neuronal injury and not gene therapy treatment, even though neuronal loss in Canavan disease has not been reported. We examined boundary effects of age by repeating our analyses after removing the first group of three older subjects or removing observations taken 40 months after treatment (by which time the maximal effects of treatment were assumed to have occurred). With all data included, the basal ganglia showed a significant treatment effect (that is, decreased NAA concentration) (Fig. 1). However, when the oldest three subjects were removed or when only earlier results (<40 months) were considered, these differences disappeared, suggesting that changes observed in the basal ganglia may be driven by the oldest patients with more advanced disease. This regional effect could also be related to previous intraventricular gene therapy in the first three subjects or could be an artifact of lowering the total number of observations with post hoc analysis. In all scenarios tested, there was a posttreatment decrease in NAA concentrations in the periventricular and frontal regions, which were designated treatment targets. In addition, there was a pattern of NAA increasing in all regions before treatment and then decreasing to the normal reference range after treatment (Fig. 1). The reference ranges provided for each region (yellow shading) are 95% confidence intervals (CIs) based on four reference subjects without Canavan disease aged 16 to 36 months (*10*). We also collected additional data on other brain metabolites using ^{1}H-MRS, which are presented in table S2.

Structural changes in white matter measured by T1 relaxation time

T1 relaxation time is an imaging modality that provides a quantitative measure of brain composition, which is influenced by factors such as water content and myelination. Although it is not appropriate to use T1 relaxation time as a measure of myelin content per se, it is common practice to use the T1 relaxation time to track changes in the physiological status of the brain in situations where the myelin content is believed to be changing. During the first years of life, T1 measurements drop exponentially in normal white matter to a value that is slightly larger than the adult value. However, in Canavan disease patients, the T1 decrease is

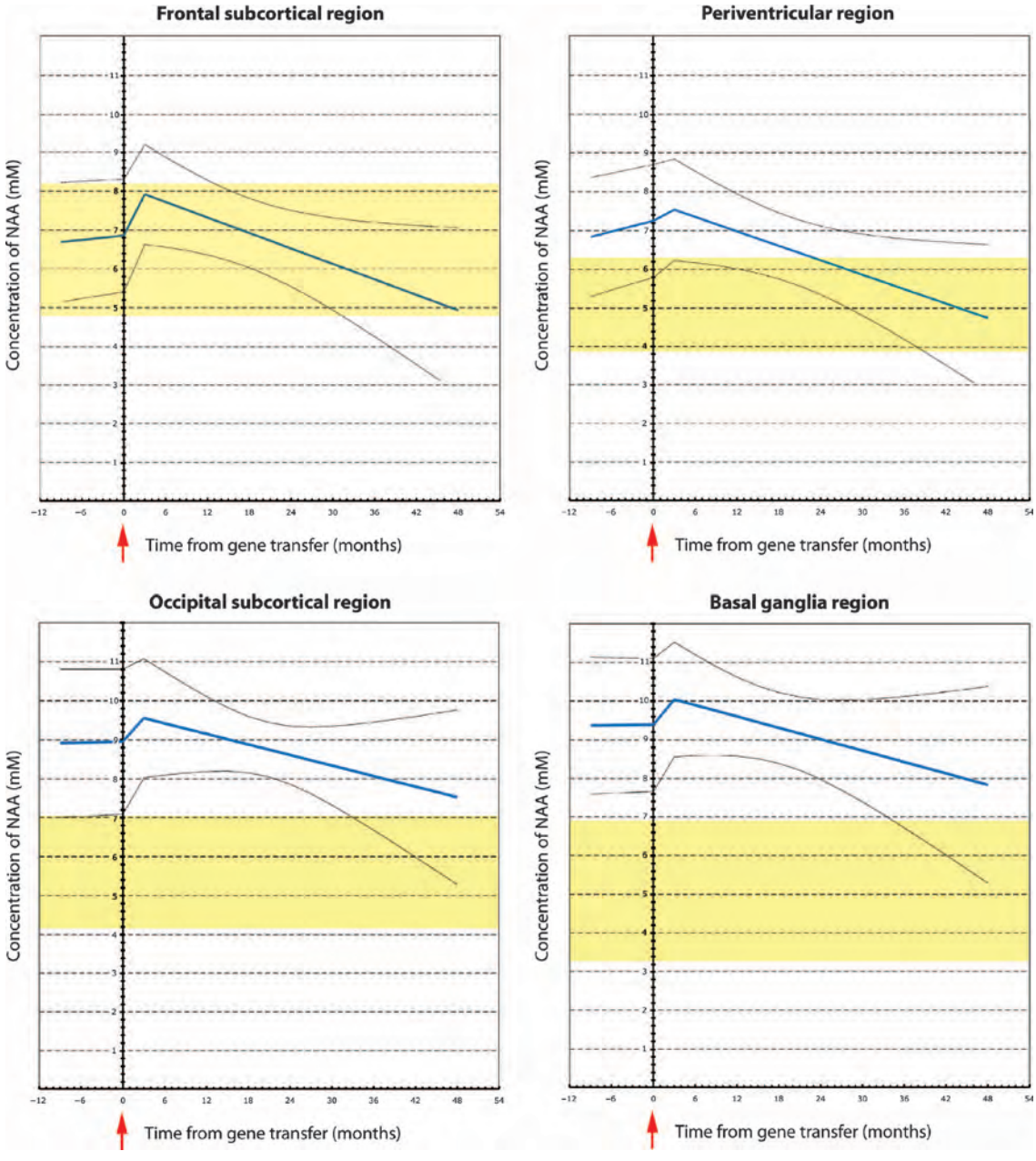

Fig. 1. Brain NAA concentrations after gene therapy (GT). Brain NAA concentrations were measured using ^{1}H-MRS in four brain regions after AAV2-*ASPA* gene therapy in 13 patients with Canavan disease. The best-fit line for NAA with the linear mixed model is shown in blue (95% CIs shown by gray lines). The normal NAA concentration reference range is shown in yellow for age-matched subjects without Canavan disease. A ramp function was fit to model the transient increase in NAA concentration that occurred in all patients before surgical administration of AAV2-*ASPA*. The greatest apparent treatment effect was in the periventricular region, which demonstrated a statistically significant decrease in NAA concentration over time (Wald statistic, $P < 0.0001$).

linear (when it occurs at all) and remains elevated over the entire period of postnatal myelination (*10*).

Here, we have used the magnitude of changes in T1 relaxation time as a general indicator of region-specific effects in the brains of subjects with Canavan disease before and after gene therapy (table S3). We obtained T1 data from 28 patients with Canavan disease, of which 13 were ultimately treated with gene therapy. In previous work, using a comparison with control data from 89 age-matched normals (*10*), we had established that the natural history of Canavan disease involves an abnormal increase in T1 relaxation time. T1 relaxation times in various brain regions of interest were an exploratory outcome measure and were more variable compared to NAA concentrations measured by spectroscopy. Because the study was powered for NAA analysis, this endpoint was considered semiquantitative.

After AAV2-*ASPA* gene therapy, the largest change in T1 was in the splenium of the corpus callosum, a large white matter tract (table S3). There was a change from a positive to a negative slope in 10 of 13 subjects, hinting at a more normal pattern of myelination (table S3). The

Table 2. NAA concentration changes by brain region. Best-fit slopes of measured NAA concentration per voxel were compared with respect to the time of treatment to look for changes in NAA concentration in different brain regions after gene therapy. All data were considered separately by region and coefficients for before treatment (pre versus zero) and after treatment (post versus zero) as well as the pre/post difference (post versus pre) are shown. Values in the top section of the table represent 13 of 13 treated subjects, and values in the bottom section of the table represent 10 of 13 subjects, with the three oldest subjects removed. Analysis using a general linear mixed model showed statistically significant changes in NAA concentrations in multiple regions. *$P < 0.05$, **$P < 0.001$.

Brain region	Pre versus zero		Post versus zero		Post versus pre	
	Coefficient	*P*	Coefficient	*P*	Difference	*P*
Frontal	+0.022	0.049*	−0.040	0.0039**	−0.062	0.0008*
Periventricular	+0.050	0.000003**	−0.032	0.065	−0.082	0.00012**
Occipital	+0.014	0.126	−0.023	0.206	−0.037	0.065
Basal ganglia	+0.009	0.318	−0.067	0.0005**	−0.86	0.00049**
Frontal	+0.018	0.183	−0.066	0.025*	−0.084	0.025*
Periventricular	+0.046	0.002*	−0.062	0.043*	−0.108	0.003**
Occipital	+0.005	0.641	−0.045	0.255	−0.50	0.220
Basal ganglia	+0.002	0.880	−0.049	0.222	−0.51	0.235

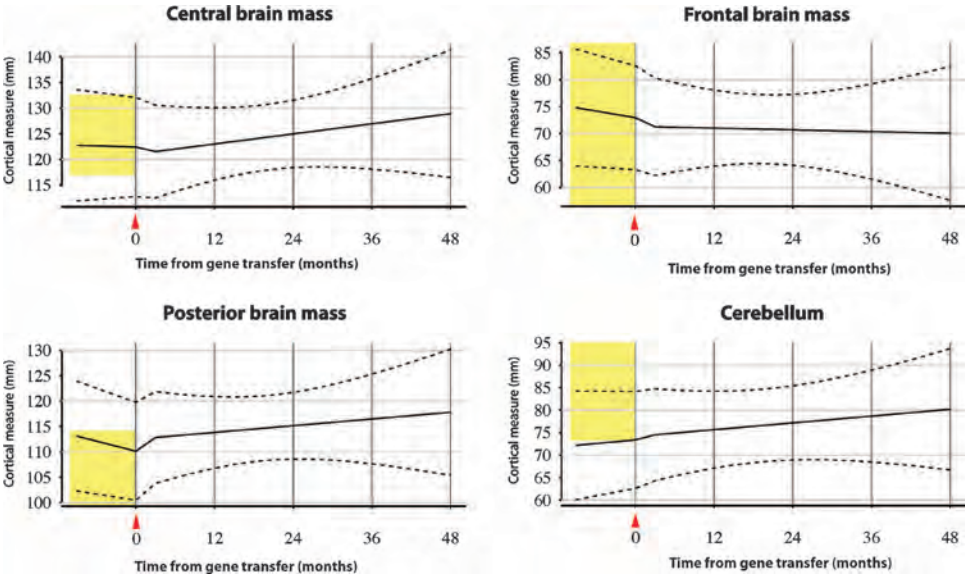

Fig. 2. Brain atrophy measurements in Canavan disease patients after gene therapy. Brain atrophy was modeled from serial measurements of predefined landmarks using the linear mixed model approach in 13 patients with Canavan disease after AAV2-*ASPA*. Brain regions included the center of the third ventricle and thalami (central brain mass), the frontal lobes (frontal brain mass), the posterior horns of the lateral ventricles and parietal-occipital lobes (posterior brain mass), and the fourth ventricle and cerebellar cortex (cerebellum). Mean cortical mass is fit to the solid black line with the linear mixed model, and variability is shown with 95% CIs (dashed lines; SD, 6.00 mm). Normal reference range (vertical yellow bar), with 95% CIs, is shown for age-matched patients without Canavan disease.

three subjects who did not show a reversal were patient 01-118-01, who had significant pretreatment brain atrophy, and patients 01-118-12 and 01-118-15, who had severe disease. A similar pattern was seen in the semiovale region (the largest subcortical white matter tract) in 8 of 13 subjects and in the parietal white matter (table S3). In other brain regions (for example, internal capsule, U fibers, and brainstem), T1 slopes remained static or increased, suggesting increased water content and/or decreased myelination. The pons and brainstem, which were farthest removed from the physical effects of gene transfer, showed the most abnormal pattern. Interpretation of T1 changes was complicated in light of multiple comparisons for different regions of interest.

Brain atrophy in Canavan disease patients after gene therapy

Serial MRI-based measures of brain atrophy were obtained from 13 Canavan disease patients receiving AAV2-*ASPA*, with calculation of the extent of ventricular enlargement and cross-sectional dimensions in predefined brain slices. To assess brain atrophy in Canavan disease subjects, we selected anatomical landmarks incorporating the ventricular spaces, which could be reproducibly assessed in cross-sectional views among all subjects. The landmarks were identified in each subject's MRI images and measured with digital image processing tools (*10*). Although brain atrophy occurred in conjunction with ventriculomegaly, these results track linear measurements of cortical and subcortical thicknesses rather than just ventricular size. We found that brain atrophy in the posterior region, encompassing the splenium of the corpus callosum and the posterior horns of the lateral ventricle, showed statistically significant changes with respect to expected values, with a reversal in the overall negative slope of brain mass (Fig. 2 and Table 3). The mean number of per-patient pretreatment observations was 2.46 and that of posttreatment observations was 4.54. The total number of patient-observation-regions was 128 for before treatment and 236 for after treatment.

The pattern of anatomical development in Canavan disease is normal growth of macroscopic brain structures and onset of myelination early in infancy (0 to 6 months), followed by gradual vacuolation of white matter and hydrocephalus, which typically accelerates after 12 months of age in untreated subjects as NAA concentrations rise. Because whole-brain increases in NAA concentrations in untreated subjects are observed alongside progressive tissue loss with hydrocephalus and cystic vacuolization, any observed decreases in NAA concentration after gene therapy cannot be explained as neuronal loss. Some subjects receiving AAV2-*ASPA* gene therapy exhibited a partial arrest or even reversal of gross brain atrophy, which was statistically significant in posterior brain regions (Fig. 2). Unfortunately, some subjects had a profound increase in gross brain atrophy before gene therapy, which may have abrogated treatment effects even as NAA concentrations became lower. For example, patient 01-118-01 showed acceleration of atrophy in the frontal, temporal, and parietal-occipital brain mass before gene therapy, which partially stabilized in frontal regions after treatment but otherwise progressed (Fig. 3).

In the posterior region, brain mass of Canavan disease patients starts at the upper end of normal, which probably reflects megaloencephaly at baseline with large posterior ventricles. As the disease progresses, microscopic spongiform changes progress to hydrocephalus ex vacuo, with significant loss of white matter. The imaging data in some patients such as 01-118-08 show a stabilization of this effect after gene therapy (Fig. 4). Aggregate data from all 13 treated patients also support a stabilization of brain atrophy (Fig. 2). Control measurements from a small reference group of non-Canavan disease patients (16 to 35 months) are shown for the same brain regions (Fig. 2). The central brain region, measured at the level of the third ventricle, as well as the frontal region and posterior fossa all demonstrated a reversal of slope, but the result was less pronounced. The cerebellum was not a target of gene therapy, and brain mass remained at the lower end of normal, which reflects gross cerebellar tissue loss and ventriculomegaly of the fourth ventricle (Fig. 2). Although the posterior region was the only one demonstrating a statistically significant change with subjects considered altogether, the trends by region are shown for individual subjects with LOESS locally linear regression (fig. S2) and suggest a variable amount of regional and subject-specific stabilization (*56*).

Table 3. Brain atrophy changes by brain region. Gross brain atrophy was assessed in four regions, three of which (frontal, central, parietal) were primarily targets of gene therapy, with the fourth region (cerebellum) located far from the treatment sites. These data represent slopes of brain mass measured at selected locations before (pre) and after (post) gene therapy. *$P < 0.05$, **$P < 0.001$.

Brain region	Pre versus zero		Post versus zero		Post versus pre	
	Coefficient	*P*	Coefficient	*P*	Difference	*P*
Frontal	−0.221	0.0002**	−0.063	0.717	0.158	0.326
Central	−0.078	0.196	+0.142	0.412	0.221	0.171
Parietal	−0.345	<0.0001**	+0.070	0.684	0.415	0.010*
Cerebellar	+0.082	0.178	+0.104	0.549	0.022	0.890

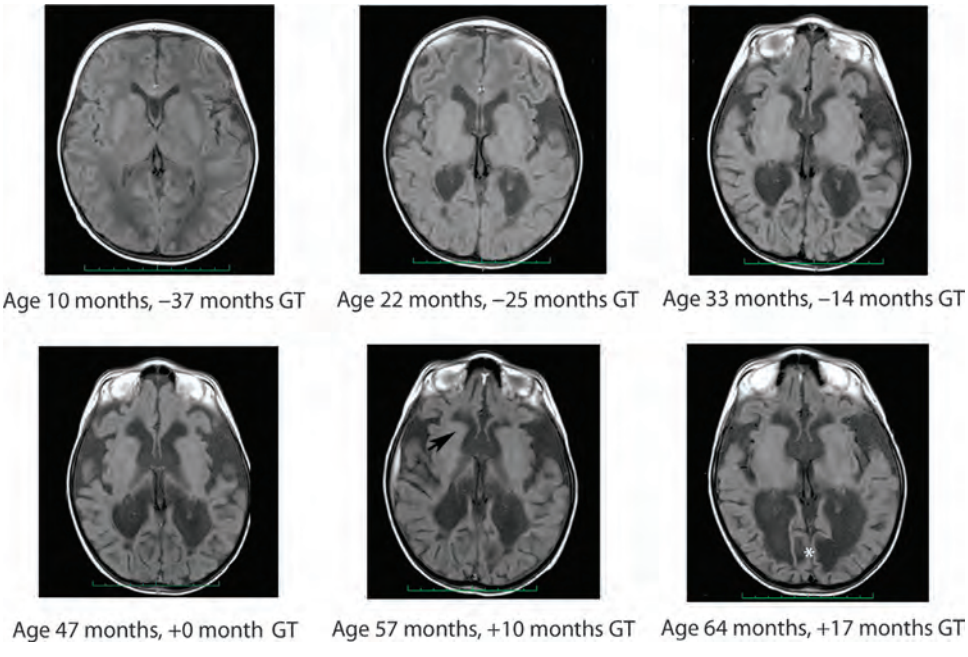

Fig. 3. Brain atrophy progression before gene therapy. Representative MRI images from patient 01-118-01 demonstrate that there was clinically significant progression of brain atrophy before AAV-*ASPA* gene therapy in some patients. In patient 01-118-01, brain atrophy was evident 3 years before gene therapy (−37 to 0 months) and may have contributed to variable treatment response. This patient was considered to be a poor responder. After gene therapy, MRI images show relative stability of brain mass around the frontal horns (black arrow) but with continued progression of encephalomalacia in the occipital region (white asterisk). Brain atrophy at selected regions is shown elsewhere on a per-subject basis (fig. S2) and altogether (Fig. 2).

Clinical outcomes in Canavan disease patients after gene therapy

The Gross Motor Function Measure (GMFM) is a standardized instrument to assess changes in gross motor function over time in the pediatric population, which has been validated in cerebral palsy and head injury patients (*57*). It is designed to assess how much of an activity a child can accomplish, rather than the quality of the motor performance, across five dimensions: lying/rolling, sitting, crawling/kneeling, standing, and walking/running/jumping. Because Canavan disease is characterized by severe truncal hypotonia and instability, lack of head support, and limb spasticity, prospectively, we focused on the lowest three functional categories as goal areas. Characteristics evaluated in this assessment include the child's ability to roll from prone to supine and to perform tasks while maintaining a supine or some version of prone position and also elements of head control, which is severely affected in Canavan

Fig. 4. Stabilization of brain atrophy in younger patients after gene therapy. Representative MRI images from Canavan disease patient 01-118-08 after AAV2-*ASPA* gene therapy. The MRI images of this younger subject, who did not have brain mass loss before gene therapy and was classified as a better responder, reveal stabilization of hydrocephalus in the frontal horn region (white arrow) and third ventricle (black arrow), as well as retention of brain mass in the frontal and posterior parietal regions.

disease. Using the generalized linear mixed model approach, we found a small but statistically significant improvement in the lying/rolling subscale of GMFM after treatment, in terms of pre/post differences (difference, +1.50; $P = 0.017$) (fig. S3). When the first group of the three older subjects was excluded, differences were significant (difference, +2.34; $P = 0.0008$), suggesting that subjects who were oldest at the time of treatment had relatively less gross motor improvement. Overall, we found that 9 of 13 subjects had an improvement or were stable in the lying and rolling subscale, and 4 of 13 declined (fig. S3). The mean age of patients receiving gene therapy who improved or remained stable was 41 months compared to 46 months for those who did not improve or declined. In terms of comparison with normative data, despite observed clinical improvements, raw scores still fell within the range for patients severely affected by spastic quadriplegia.

The Canavan physical exam consisted of clinical findings graded by a neurologist and compared to the previous visit's clinical exam before gene transfer. The exam also incorporated narrative comments from caregivers as part of quality-of-life assessments. Specific outcomes included level of alertness, head lag, optic atrophy, cranial nerve exam, ability to fix on objects, visual tracking, truncal and extremity tone, spontaneous movement of extremities and fine motor function, sensory exam, and reflexes. The level of alertness was based on sustained interactions over a 45-min exam and was measured on an ordinal scale from 0 to 3, with interactions graded as severely diminished, moderately diminished, mildly diminished, or appropriate for age. Considering all subjects together, there was an increase in alertness level that was not statistically significant for all subjects using the generalized linear mixed model at 48 to 60 months (difference, +0.31; $P = 0.13$) (fig. S4). However, when the oldest subjects were removed, there was a significant difference in the level of posttreatment alertness (difference, +0.62; $P = 0.002$) without a change in slope, which appears related to the discrete nature of the rating scale and implies that younger subjects had somewhat better response. Overall, we found that 10 of 13 subjects had a favorable change in alertness scale (fig. S4). The three oldest patients had no change or got worse, but the other patients improved. Although individual patients showed improvement in their visual tracking and motor skills, these were not statistically significant when considered for the entire group. The Ashworth spasticity scale was scored at each visit on an ordinal scale from 1 to 5 (that is, normal tone to rigidity). A significant change in rigidity after gene therapy for all subjects considered together was not detected (fig. S5). However, when the first group was again excluded, there was a trend toward clinical improvement in spasticity of the lower extremities (difference, −0.32; $P = 0.09$) (fig. S5).

The Pediatric Inventory of Disability Index (PEDI) is a standardized functional assessment scale for disabled children, which measures capability and performance of functional activities in the following three domains: self-care, mobility, and social function (*53*). Using the generalized linear mixed model, we were not able to detect statistically significant changes with respect to the time of treatment in the self-care or mobility domains of PEDI. However, the social function domain showed a statistically significant improvement at 18 months ($P = 0.04$) (fig. S6). This effect was not significant when repeated with aggregate data at the 48- to 60-month time points, suggesting an early but nondurable behavioral effect of treatment. The other psychometric assessment, the Mullen Scales of Early Learning, is a comprehensive, standardized measure of cognitive function that comprises five scales of gross motor, visual reception, fine motor, receptive language, and expressive language (*58*). The difference in overall level of receptive language score increased but was not statistically significant after 24 months (difference, +0.23; $P = 0.83$), and that of expressive language score decreased but was also nonsignificant (difference, −0.77; $P = 0.29$) (fig. S7). On the basis of normative values, treated subjects who had their final Mullen assessments between the ages of 10 and 108 months (mean, 53 months) attained maximal age-equivalent scores of 4 to 6 months for gross and fine motor, 2 months for visual receptive, 9 months for expressive language, and 15 to 17 months for receptive language.

As part of clinical monitoring, a clinical seizure inventory and medication log was compiled for each of the 13 patients receiving AAV2-*ASPA* gene therapy. Electroencephalograms (EEGs) were not routinely incorporated into posttreatment assessments, but subjects had EEGs if clinically warranted. The untreated subjects were followed for brain NAA concentrations and at least one standardized neurological assessment, but seizures were not followed. Of the patients who received gene therapy, 9 of 13 (69%) had a previous clinical seizure history, which was documented for at least 12 months before enrollment or from birth. Only 3 of 13 (23%) patients had multiple severe myoclonic or generalized tonic-clonic seizures in the previous 12 months (Table 1). Among those with a clinical seizure history, nine of nine were on acetazolamide, four of nine were on clonazepam, three of nine were on oxcarbazepine, three of nine were on phenobarbital, and one of nine was on valproic acid. For antispasmodic treatment, 4 of 13 subjects were on baclofen or tizanidine. Two of the 13 treated subjects had no seizures either before or after gene therapy (patients 01-118-08 and 01-118-12) (fig. S8). After treatment, 11 subjects exhibited a decrease in clinically evident seizure frequency or continued to have no seizures at all, and two worsened or had new seizures (patients 01-118-24 and 01-118-33) (fig. S8). Both of the subjects who worsened had no previous seizure history and had not taken prophylactic antiseizure medications before gene therapy. One of them, subject 01-118-24, developed new seizures after surgical complications of a brain abscess and bilateral subdural hematomas. After

starting antiepileptic medications (levetiracetam), seizures in both subjects were well controlled.

Patients with Canavan disease exhibit a variety of seizure types, and we distinguished clinically between absence-like seizures, consisting of short episodes of eye blinking and staring spells with an abnormal EEG background, and myoclonic or generalized tonic-clonic seizures. The incidence of clinically evident seizures before and after gene therapy was compared against the null hypothesis of no overall change. Among the 13 treated subjects, two had no clinically evident absence-like seizures before or after gene therapy, nine had a decrease, and two had an increase in the mean seizure frequency (fig. S8). For myoclonic/tonic-clonic seizures, nine patients had none in pretreatment screening and after gene therapy, and the other four patients showed improvements in these seizures (fig. S8). Using generalized linear mixed models, which allow for subject-specific parameter values, with Poisson and binomial distributional families, this decrease in seizure frequency was significant ($P < 0.001$) for both absence-like and myoclonic or tonic-clonic seizures (fig. S8). In particular, all three subjects with refractory seizures (patients 01-118-02, 01-118-05, and 01-118-15) experienced a decrease in symptoms of epilepsy after treatment. Subject 01-118-02 had a history of frequent generalized seizures and was taking acetazolamide and oxcarbazepine. After gene transfer, the frequency of absence-like seizures decreased for at least 60 months, with a single isolated episode of myoclonic seizures, which occurred at the time of a hospitalization for gastric feeding tube placement. Subject 01-118-05 was taking acetazolamide, oxcarbazepine, and phenobarbital for frequent absence-like and myoclonic seizures, which decreased in frequency starting in the 12 months postoperatively and permitted discontinuation of phenobarbital. Subject 01-118-15 had a history of refractory seizures and was taking acetazolamide and clonazepam; the overall frequency was five seizures with sustained myoclonus in the year preceding gene transfer and only one seizure in the year after gene transfer, with a concurrent reduction in clonazepam. For subjects who experienced infrequent absence-like seizures, five of six (83%) have been entirely seizure-free after treatment for at least 60 months, with a decrease in seizure medications in four of six (66%).

Outside of the hospitalization period, study investigators did not clinically manage individual subjects, who remained under the care of their own pediatricians and neurologists after hospital discharge. Therefore, primary responsibility for clinical monitoring and adverse events reporting after the hospitalization phase fell upon the parents and outside consultants. However, we closely followed the number and dosing of medications, which were titrated by outside physicians on the basis of each patient's individual clinical status. Given the variety of medications used in practice and the small number of subjects, we did not convert to equivalent doses of a "standard" antiepileptic regimen. Instead, we followed changes in the number or dosing of agents for each subject before and after gene therapy. To minimize observer bias, we did not inform treating physicians that we were monitoring their medication titration. In addition to the observed decrease in clinical seizure frequency in 11 of 13 subjects, we found that 8 of 13 subjects (61%) had a simultaneous decrease in their antiepileptic medications. Moreover, all four subjects (100%) on antispasmodics decreased or discontinued baclofen or tizanidine due to improvements in resting tone.

Adverse events in Canavan disease patients 90 days after gene therapy

The complete adverse events within 90 days of surgery to administer gene therapy is shown (Table 4). Treatment with AAV-*ASPA* was associated with two serious adverse events based on the current FDA definition. One serious adverse event (01-118-004) was graded mild and consisted of a postoperative low-grade fever, responding to antipyretics, leading to a 24-hour prolongation of hospitalization. The other (01-118-24) was graded severe and consisted of a postoperative brain abscess and bacteremia. Both events were determined to be unrelated to AAV-*ASPA* gene therapy. Postoperative fever occurred in most subjects but was self-limiting and responded to antipyretics. In addition, most subjects experienced a small hemorrhage associated with the passage of the borosilicate delivery catheter for AAV-*ASPA* into the subcortical white matter. In most cases, any hemorrhage was small and self-limiting, but two subjects experienced bilateral chronic subdural hematomas. These resolved on their own and have not required surgical drainage. During the course of longer-term monitoring, no additional adverse events were reported in post-hospitalization surveillance over a minimum period of 5 years, in some cases up to 10 years. Hospitalizations or medication changes were brought to the attention of the study sponsor, but none (aside from decreases in antiepileptic usage) were found to be related to gene therapy. Seven of 13 subjects were hospitalized for elective surgical procedures such as gastric feeding tubes. Other hospitalizations were for routine issues such as ear infections, pneumonia, electrolyte management, or medical issues not related to gene therapy. Subject 01-118-007 developed hydrocephalus 10 years after gene therapy and was hospitalized for shunt placement, which was complicated by iatrogenic surgical hemorrhage. All subjects (except for two who withdrew after the 60-month clinical follow-up) remain under clinical surveillance and all subjects are alive at the time of writing, with an age range of 6 to 17 years.

DISCUSSION

This study using AAV2-*ASPA* gene therapy for treating Canavan disease reports 10 years of safety data with a minimum clinical monitoring interval of 5 years for all subjects. There were no adverse events after the 90-day postoperative period. Immune responses to AAV2 appeared limited and have been previously reported (*59*). Brain NAA concentrations, our primary outcome measure, showed decreases after treatment and approached normal NAA concentrations in the non-Canavan reference range. In previous work (*60*), we examined a mixed population of normal patients aged 1 to 31 years, looking specifically at the basal ganglia region, and found a mean NAA value of 5.8 mM across this age range (95% CI, 4.7 to 6.9 mM), which compares well with the current values. Another quantitative metabolite study (*61*) looking at multiple brain regions in normal pediatric subjects examined 15 subjects, aged 3 months through 19 years, and found a mean NAA concentration of 7.9 mM (range, 6.9 to 8.6 mM) across nine brain regions. Another group (*62*) measured quantitative NAA during development in 50 subjects from birth to 18 years, who were scanned for a variety of reasons, and found that NAA concentrations in occipital gray matter (where NAA is highest) asymptotically peaked around 4 years of age at about 8.8 mM, with no further changes into adulthood. These data suggest that there is no significant increase in mean NAA concentrations from toddler age to adulthood during normal development, and the normal NAA range in healthy subjects is relatively static. In contrast, subjects with Canavan disease show a dynamic pattern of increasing NAA before treatment and decreasing NAA after gene therapy.

Although secondary outcome measures were not designed to be definitive, there was evidence of positive radiographic and clinical changes,

Table 4. Adverse events within 90 days of gene therapy. Adverse events in 13 Canavan disease subjects 90 days after AAV2-*ASPA* gene therapy are listed by category, with notation of serious adverse events (*). Because of the small sample size and rarity of adverse events, analysis was performed with Fischer's exact method to calculate expected frequencies. For events with zero incidence, Agresti-Coulli intervals are provided.

Clinical finding	Group 1	Group 2	Group 3	Incidence (%)	95% CI
Fever (postoperative)	1/3*	4/7	1/3	46	0.192–0.749
Emesis (postoperative)	1/3	0/7	0/3	8	0.002–0.360
Seizures (postoperative)	1/3	0/7	0/3	8	0.002–0.360
Subarachnoid hemorrhage, mild	0/3	2/7	3/3	38	0.139–0.684
Subdural hemorrhage (<1 cm)	0/3	4/7	3/3	54	0.251–0.808
Soft tissue inflammation, extracranial	0/3	2/7	1/3	23	0.050–0.538
CSF leak	0/3	1/7	2/3	23	0.050–0.538
Hydrocephalus requiring shunt	0/3	0/7	0/3	–	0–0.247
Immune reaction, rash/urticaria	1/3	0/7	1/3	15	0.019–0.455
Immune reaction, other, local	0/3	0/7	1/3	8	0.002–0.360
Immune reaction, other, systemic	0/3	0/7	1/3	8	0.002–0.360
Superficial wound infection	0/3	0/7	0/3	–	0.002–0.360
Brain abscess, cerebritis, or meningitis	0/3	0/7	1/3*	8	0–0.247
Anemia, mild	2/3	0/7	0/3	15	0.019–0.455
Respiratory infection, mild	2/3	0/7	0/3	15	0.019–0.455
Pulmonary, other	0/3	0/7	0/3	–	0–0.247
Cardiovascular	0/3	0/7	0/3	–	0–0.247
Renal	0/3	0/7	0/3	–	0–0.247
Endocrine	0/3	0/7	0/3	–	0–0.247
Gastrointestinal	0/3	0/7	0/3	–	0–0.247
Genitourinary	0/3	1/7	0/3	8	0.002–0.360
Clinical chemistry, change from baseline	0/3	0/7	1/3	8	0.002–0.360

which will need to be validated in a larger clinical trial. Together with significantly reduced NAA concentrations in the frontal and periventricular regions, evidence for a regional effect of gene therapy includes T1 normalization in the splenium of the corpus callosum, suggesting increased myelination and/or decreased water content. The same anatomical region showed a relative stabilization of brain atrophy, although variability among subjects in the timing and rate of change of pretreatment disease progression complicated the analysis. There are several components to brain atrophy that cannot be easily separated with imaging, including reversal of hydrocephalus, slowing of the rarefaction of gross brain mass, and creating a milieu that permits some degree of normal myelination. We propose that one possible mechanism for stabilization of brain atrophy is decreased hydrocephalus and slowing in the rate of decay of white matter tracts as the brain went through an age-dependent increase in mass. When this study started 11 years ago, a viral vector that specifically targeted oligodendrocytes was not available. AAV2 was the safest and most effective gene transfer vector but is limited to expression of the therapeutic gene in neurons only (*63*). We hypothesized that spongiform degeneration would be slowed or prevented if pathologically high NAA concentrations were decreased and global NAA in the extracellular space was diminished through expression of aspartoacylase in neurons. One assumption was that osmotic, metabolic, or epileptogenic effects of NAA and NAAG would prove to be as important as any biosynthetic role of NAA in myelin synthesis. Another assumption was that elevated neonatal NAA would not have permanently disrupted the myelination program or oligodendrocyte migration before gene transfer was performed, given that *ASPA* has been implicated in these processes. Developmental processes affected by NAA during myelination, such as early migration and differentiation of oligodendrocytes, may be an important consideration in the timing of gene therapy. It is desirable for newer gene therapy vectors to target oligodendrocytes or a mixed neuronal-glial cell population. Future studies of Canavan disease will probably use alternative AAV serotypes. Other issues to be addressed include the need for less invasive delivery of the vector and its therapeutic gene (fig. S9), such as endovascular approaches. A major limitation of our study is that it was not possible to target the cerebellum or brainstem, which is physically separated from supratentorial sites of gene transfer. There is cerebellar and brainstem pathology in Canavan disease, and ASPA is normally expressed in the cerebellar white matter (*25*, *64*). Because the cerebellum coordinates motor behavior, it is possible that clinical gains in the motor domain are limited by pathology in the posterior fossa.

Part of the complexity of Canavan disease is that NAA may have a number of separate and overlapping roles that differ from fetal to adult life. The pathology of elevated periaxonal NAA is likely to be multifactorial, involving osmotic, metabolic, and lipid biosynthetic effects

on glia; epileptogenic effects on neurons; and developmental effects from altered induction of the myelination program. The excitotoxic effects of NAA are still poorly understood in vivo and have been recently discounted (*65*), although NAA and NAAG were reported to activate *N*-methyl-D-aspartate (NMDA) receptors at millimolar concentrations (*66*, *67*). NAA in extracellular fluid or cerebrospinal fluid (CSF) is associated with seizures in both humans and the tremor rat model of Canavan disease (*41*, *42*). This effect is reproduced by administering high concentrations of NAA to normal rats (*68*), which suggests that NAA may be excitotoxic in vivo under certain circumstances. One notable clinical feature was the relative decrease in seizure frequency in gene therapy–treated subjects, which was also reported in the tremor rat model of Canavan disease after AAV2-*ASPA* gene therapy (*69*).

NAA is required for some components of myelin synthesis, but alternative biosynthetic pathways for myelin occur during development. Evidence suggests that a failure to produce normal myelin, combined with an increase in interstitial NAA that affects myelin integrity, makes the proper maintenance of myelination impossible. Some have proposed a primary role of NAA in myelin synthesis and argue that hypomyelination from inadequate production of acetate by aspartoacylase in oligodendrocytes is the main cause of Canavan disease. However, myelin is produced in Canavan disease patients and *ASPA* null rodent models, indicating that NAA is not the sole acetyl source for lipid biosynthesis. NAA is not absolutely necessary for myelination, and a case study of a child without any NAA showed only moderately delayed myelination (*70*). The aberrant myelination in the tremor rat model of Canavan disease is characterized by selective increases as well as decreases in lipids, with early reduction in sulfatides and cerebrosides and up-regulation of specific species of phosphatidylcholine (*33*). Chemical analysis in patients with spongy degeneration suggests a relative imbalance in phosphatides and cerebrosides, with low proteolipid and glycolipid levels (*71*). Of special relevance is the fact that aspartoacylase is required for synthesis of cerebronic acid from lignoceric acid (*30*), which suggests that cerebroside augmentation may thwart dysmyelination. Lack of bioavailable acetate is unlikely to be the key feature of Canavan disease (*72*), and proposed acetate supplements (*73*) may also require reduction in pathologically elevated NAA for any beneficial effect to occur.

Normalization of NAA at a very early age may be necessary to prevent irretrievable dysmyelination, motor delay, and mental retardation in Canavan disease. Recent clinical studies of neurometabolic diseases such as globoid cell leukodystrophy and mucopolysaccharidosis have shown a disproportionate response to very early interventions (*74*, *75*), with the therapeutic window often closing in a matter of weeks after birth. Although AAV-*ASPA* delivered between 4 and 83 months appears to change the typical radiographical progression of disease, our data suggest that an earlier time window probably exists for effective treatment. Subjects who experienced the greatest magnitude of positive changes in quality-of-life measures were treated before 2 years of age. These early age effects included improvement in attention and sleep-waking cycles, titration of seizure medications with stable epilepsy, and greater magnitude of motor improvements in lying and rolling. Older patients invariably presented with greater brain atrophy, which may have contributed to less clinical improvement than seen in younger patients. Future gene therapy interventions for Canavan disease should focus on the neonatal age range (0 to 3 months) before irreversible structural changes have occurred, using newer vectors that target oligodendrocytes or a mixed target cell population including glia, neurons, and arachnoid cells. Unfortunately, diagnosis typically does not occur until 12 months of age, after patients have already lost developmental milestones; thus, early diagnosis and intervention are essential.

MATERIALS AND METHODS

Surgical procedure

Gene therapy took place in the operating room under general anesthesia. After induction of anesthesia, subjects were placed into an age-appropriate rigid head support and secured to the operating table with a moderate degree of head flexion. Six burr hole sites were identified, and the head was prepared in standard sterile fashion. Incisions were made bilaterally in the frontal, parietal, and occipital regions. A pneumatic perforator was used to make burr holes. The dura was cauterized and incised. After the pia was opened, preprimed borosilicate catheters were introduced to the brain under direct visualization to a subcortical depth of 2 cm and secured in place with sterile adhesive tape (fig. S9). The initial 10 patients had freehand placement of infusion cannulas, and the last three patients had stereotactic placement. Using a microperfusion pump, we injected 150 μl of AAV-ASPA vector at a standardized titer of 1×10^{12} genomic particles per milliliter simultaneously to each of the six sites at a rate of 2 μl/min (infusion time, 75 min), for a total delivery volume of 900 μl and total unit dose of 900 billion genomic particles of AAV-ASPA.

Imaging

MRI and ^{1}H-MRS imaging data were collected at Children's Hospital of Philadelphia with a Siemens 1.5-T magnet with a standard head coil. Acquisition parameters have been described (*10*). ^{1}H-MRS examinations were performed with the single voxel STEAM method. The voxel positioning was guided with the graphical interface of the scanner. After the water-suppressed measurement, the water signal from the same voxel was measured with T_R = 5000 ms. Data were acquired in four areas of interest, and signal calibration was done with a phantom replacement technique in which the metabolite concentrations in the spectra were obtained by fitting the in vivo brain absorption spectra as linear combinations of individual metabolite spectra.

Data analysis plan

All data were collected in a secure clinical database according to our protocol (*48*) and exported for data analysis. Data were prospectively fit to a generalized linear mixed model, the preferred method for repeated-measures within-subject data, as well as longitudinal cohort data (*51*). The study was powered for efficacy on the basis of previous clinical data (*47*), with brain NAA concentrations as the variable of interest. Using 0.5 as the SD of differences in a two-tailed, 5% paired *t* test, a sample size of 15 gave power exceeding 99% for differences in NAA concentrations of 2 to 3 mM. Although this analysis suggested that a smaller sample size was sufficient, we anticipated multiple comparisons and the possibility of patient attrition and originally planned to enroll and treat 21 subjects (*48*). However, our planned interim analysis indicated that data from 13 treated subjects would be sufficient for comparing primary outcome measures of NAA and clinical adverse events, and the Independent Data Monitoring Committee recommended modification of the protocol to 13 treated subjects with a plan for dose escalation in future phase 2/3 studies. Our planned analysis also incorporated longitudinal data from 15 untreated Canavan disease subjects as part of the generalized linear mixed model. Apart from these changes in study design, the data analysis plan was previously reported (*48*). In general, the data analysis

strategy for longitudinally assessed measures was to fit mixed-effect models with random intercept, age, and time posttherapy effects for each subject. The linear mixed-effect model is of the general form $Y_i = X_i\beta + Z_i b_i + \varepsilon_I$, where X_i and Z_i are the respective covariate matrices for fixed and random effects, β is the coefficient for fixed effects, and b_i and ε_I are random errors. This mixed-effect model is commonly used for applications involving longitudinal data, where Y_i are repeated measures over time of a particular response variable and measurement times are included in the matrices. Without assuming specific forms for X_i and Z_i, the model is capable of handling time-dependent covariates, unequally spaced responses, and incomplete data. With NAA data, this model fits a piecewise linear function with one joint at the time of therapy and one joint 3 months later to account for surgery effects, with subject-specific slopes both before and after the therapy. To study the effect of treatment within a region, we included interactions of age and time posttherapy with region. Statistical significance of each coefficient was evaluated by examining the Wald statistic, the estimate of the coefficient divided by its estimated SE. For statistical treatment of various clinical and cognitive outcomes, several of the outcomes were not continuous but instead were dichotomous, ordinal, or categorical. In measures with sufficient variation, the standard random effects model was replaced by generalized estimating equations that are better suited to noncontinuous outcomes. This model is analogous to the piecewise linear model defined for continuous measures but has a different distributional family structure for the residuals. For generalized linear mixed models, we used the R Project for Statistical Computing packages nlme and lme4.

Vector production

The construction of the *ASPA* gene cassette, AAV2 preparative methods, and preclinical testing have been previously described (*10*, *48*). Clinical grade AAV2 vector was produced in core facilities at the University of Auckland (lot 1) and the University of North Carolina (UNC; lots 2 and 3) with predefined criteria for quality control. The three treatment groups correspond to separate lots of AAV-ASPA, which was necessary due to Good Manufacturing Practice requirements. Clinical grade vector was tested for purity and potency according to Investigational New Drug Protocol IND-9119. Although preclinical studies in neonatal primates had established the tolerability of 2.4×10^{10} genomic particles AAV2 per gram of brain, the FDA stipulated a 35-fold lower unit dose of 7×10^8 genomic particles per gram of brain in human subjects. Although the unit dose of 9×10^{11} genomic particles per patient may be suboptimal for maximal clinical effect, dose escalation was not a feature of this phase 1/2 clinical trial, and all patients received the same standard dose.

Procedures for data collection

Data collection consisted of imaging and clinical assessments at least twice before treatment and after treatment at 0.5, 1, 3, 6, 9, 12, and 15 months and periodically thereafter. Brain atrophy data were acquired together with NAA and T1 values and were stored on a workstation for quantitative measurements at predefined anatomical landmarks (*10*). Frontal brain mass was measured at the level of the caudate head posterior to the pericallosal vessels at the genu of the corpus callosum, central brain mass was measured at the level of the thalamus at the widest point of the third ventricle, posterior brain mass was measured across the posterior horns of the lateral ventricles at the level of the deep cerebral veins and choroid plexus, and cerebellar mass was measured across the widest part of the fourth ventricle to the borders of the venous sinuses on either side. To avoid observer bias, two radiologists independently measured the regions of interest for each subject, which was verified by a third investigator. Although there are no accepted pediatric rating scales specifically designed for leukodystrophies, we adapted tests that were developed for similar patient populations such as childhood cerebral palsy. Standardized psychometric tests and functional scales were administered by an independent child psychologist, and neurological exams were administered by a board-certified child neurologist appointed by the Independent Data Monitoring Committee. Each subject had at least two formal exams of each type before treatment, followed by serial exams at each follow-up visit. Because of the invasive surgical administration of gene therapy, the use of customized quality-of-life test questions, and the fact that this was a phase 1/2 safety study and clinical assessments were not a primary outcome measure, clinical evaluation was unblinded.

SUPPLEMENTARY MATERIALS

www.sciencetranslationalmedicine.org/cgi/content/full/4/165/165ra163/DC1
Table S1. Demographics of untreated Canavan disease subjects.
Table S2. Other metabolites from ^{1}H-MRS.
Table S3. Quantitative T1 results by brain region.
Fig. S1. Modeling of NAA by individual subject.
Fig. S2. Modeling of brain atrophy by individual subject.
Fig. S3. GMFM mean scores, pre/post gene therapy.
Fig. S4. Canavan alertness scale.
Fig. S5. Ashworth spasticity scale.
Fig. S6. PEDI social function test.
Fig. S7. Mullen expressive and receptive language tests.
Fig. S8. Frequency of seizures
Fig. S9. Surgical procedure.

REFERENCES AND NOTES

1. L. Hagenfeldt, I. Bollgren, N. Venizelos, *N*-acetylaspartic aciduria due to aspartoacylase deficiency—A new aetiology of childhood leukodystrophy. *J. Inher. Metab. Dis.* **10**, 135–141 (1987).
2. R. Matalon, K. Michals, D. Sebesta, M. Deanching, P. Gashkoff, J. Casanova, Aspartoacylase deficiency and *N*-acetylaspartic aciduria in patients with Canavan disease. *Am. J. Med. Genet.* **29**, 463–471 (1988).
3. R. Kaul, G. P. Gao, K. Balamurugan, R. Matalon, Cloning of the human aspartoacylase cDNA and a common missense mutation in Canavan disease. *Nat. Genet.* **5**, 118–123 (1993).
4. E. Bitto, C. A. Bingman, G. E. Wesenberg, J. G. McCoy, G. N. Phillips Jr., Structure of aspartoacylase, the brain enzyme impaired in Canavan disease. *Proc. Natl. Acad. Sci. U.S.A.* **104**, 456–461 (2007).
5. R. Kaul, J. Casanova, A. B. Johnson, P. Tang, R. Matalon, Purification, characterization, and localization of aspartoacylase from bovine brain. *J. Neurochem.* **56**, 129–135 (1991).
6. M. H. Baslow, R. F. Suckow, V. Sapirstein, B. L. Hungund, Expression of aspartoacylase activity in cultured rat macroglial cells is limited to oligodendrocytes. *J. Mol. Neurosci.* **13**, 47–53 (1999).
7. G. Chakraborty, P. Mekala, D. Yahya, G. Wu, R. W. Ledeen, Intraneuronal *N*-acetylaspartate supplies acetyl groups for myelin lipid synthesis: Evidence for myelin-associated aspartoacylase. *J. Neurochem.* **78**, 736–745 (2001).
8. K. K. Bhakoo, T. J. Craig, P. Styles, Developmental and regional distribution of aspartoacylase in rat brain tissue. *J. Neurochem.* **79**, 211–220 (2001).
9. C. N. Madhavarao, J. R. Moffett, R. A. Moore, R. E. Viola, M. A. Namboodiri, D. M. Jacobowitz, Immunohistochemical localization of aspartoacylase in the rat central nervous system. *J. Comp. Neurol.* **472**, 318–329 (2004).
10. C. G. Janson, S. W. McPhee, J. Francis, D. Shera, M. Assadi, A. Freese, P. Hurh, J. Haselgrove, D. J. Wang, L. Bilaniuk, P. Leone, Natural history of Canavan disease revealed by proton magnetic resonance spectroscopy (^{1}H-MRS) and diffusion-weighted MRI. *Neuropediatrics* **37**, 209–221 (2006).
11. A. Moreno, B. D. Ross, S. Blüml, Direct determination of the *N*-acetyl-L-aspartate synthesis rate in the human brain by ^{13}C MRS and [1-^{13}C]glucose infusion. *J. Neurochem.* **77**, 347–350 (2001).
12. H. H. Tallan, Studies on the distribution of *N*-acetyl-L-aspartic acid in brain. *J. Biol. Chem.* **224**, 41–45 (1957).

13. G. Tsai, J. T. Coyle, *N*-acetylaspartate in neuropsychiatric disorders. *Prog. Neurobiol.* **46**, 531–540 (1995).
14. J. R. Moffett, S. B. Tieman, D. R. Weinberger, J. T. Coyle, A. M. Namboodiri, *N-Acetylaspartate: A Unique Molecule in the Central Nervous System* (Springer, New York, 2006).
15. H. H. Tallan, S. Moore, W. H. Stein, *N*-acetyl-L-aspartic acid in brain. *J. Biol. Chem.* **219**, 257–264 (1956).
16. T. B. Patel, J. B. Clark, Synthesis of *N*-acetyl-L-aspartate by rat brain mitochondria and its involvement in mitochondrial/cytosolic carbon transport. *Biochem. J.* **184**, 539–546 (1979).
17. C. N. Madhavarao, C. Chinopoulos, K. Chandrasekaran, M. A. Namboodiri. Characterization of the *N*-acetylaspartate biosynthetic enzyme from rat brain. *J. Neurochem.* **86**, 824–835 (2003).
18. Z. H. Lu, G. Chakraborty, R. W. Ledeen, D. Yahya, G. Wu, *N*-acetylaspartate synthase is bimodally expressed in microsomes and mitochondria of brain. *Brain Res. Mol. Brain Res.* **122**, 71–78 (2004).
19. M. L. Simmons, C. G. Frondoza, J. T. Coyle, Immunocytochemical localization of *N*-acetyl-aspartate with monoclonal antibodies. *Neuroscience* **45**, 37–45 (1991).
20. J. R. Moffett, M. A. Namboodiri, C. B. Cangro, J. H. Heale, Immunohistochemical localization of *N*-acetylaspartate in rat brain. *Neuroreport* **2**, 131–134 (1991).
21. D. L. Taylor, S. E. Davies, T. P. Obrenovitch, J. Urenjak, D. A. Richards, J. B. Clark, L. Symon, Extracellular *N*-acetylaspartate in the rat brain: In vivo determination of basal levels and changes evoked by high K^+. *J. Neurochem.* **62**, 2349–2355 (1994).
22. T. N. Sager, C. Thomsen, J. S. Valsborg, H. Laursen, A. J. Hansen, Astroglia contain a specific transport mechanism for *N*-acetyl-L-aspartate. *J. Neurochem.* **73**, 807–811 (1999).
23. W. Huang, H. Wang, R. Kekuda, Y. J. Fei, A. Friedrich, J. Wang, S. J. Conway, R. S. Cameron, F. H. Leibach, V. Ganapathy, Transport of *N*-acetylaspartate by the Na^+-dependent high-affinity dicarboxylate transporter NaDC3 and its relevance to the expression of the transporter in the brain. *J. Pharmacol. Exp. Ther.* **295**, 392–403 (2000).
24. J. Urenjak, S. R. Williams, D. G. Gadian, M. Noble, Specific expression of *N*-acetylaspartate in neurons, oligodendrocyte-type-2 astrocyte progenitors, and immature oligodendrocytes in vitro. *J. Neurochem.* **59**, 55–61 (1992).
25. B. F. Kirmani, D. M. Jacobowitz, M. A. Namboodiri, Developmental increase of aspartoacylase in oligodendrocytes parallels CNS myelination. *Brain Res. Dev. Brain Res.* **140**, 105–115 (2003).
26. J. S. Francis, A. Olariu, S. W. McPhee, P. Leone, Novel role for aspartoacylase in regulation of BDNF and timing of postnatal oligodendrogenesis. *J. Neurosci. Res.* **84**, 151–169 (2006).
27. D. L. Taylor, S. E. Davies, T. P. Obrenovitch, M. H. Doheny, P. N. Patsalos, J. B. Clark, L. Symon, Investigation into the role of *N*-acetylaspartate in cerebral osmoregulation. *J. Neurochem.* **65**, 275–281 (1995).
28. M. H. Baslow, Molecular water pumps and the aetiology of Canavan disease: A case of the sorcerer's apprentice. *J. Inherit. Metab. Dis.* **22**, 99–101 (1999).
29. A. F. D'Adamo Jr., F. M. Yatsu, Acetate metabolism in the nervous system. *N*-acetyl-L-aspartic acid and the biosynthesis of brain lipids. *J. Neurochem.* **13**, 961–965 (1966).
30. H. Shigematsu, N. Okamura, H. Shimeno, Y. Kishimoto, L. Kan, C. Fenselau, Purification and characterization of the heat-stable factors essential for the conversion of lignoceric acid to cerebronic acid and glutamic acid: Identification of *N*-acetyl-L-aspartic acid. *J. Neurochem.* **40**, 814–820 (1983).
31. R. Burri, C. Steffen, N. Herschkowitz, *N*-acetyl-L-aspartate is a major source of acetyl groups for lipid synthesis during rat brain development. *Dev. Neurosci.* **13**, 403–411 (1991).
32. C. N. Madhavarao, P. Arun, J. R. Moffett, S. Szucs, S. Surendran, R. Matalon, J. Garbern, D. Hristova, A. Johnson, W. Jiang, M. A. Namboodiri, Defective *N*-acetylaspartate catabolism reduces brain acetate levels and myelin lipid synthesis in Canavan's disease. *Proc. Natl. Acad. Sci. U.S.A.* **102**, 5221–5226 (2005).
33. J. Wang, P. Leone, G. Wu, J. S. Francis, H. Li, M. R. Jain, T. Serikawa, R. W. Ledeen, Myelin lipid abnormalities in the aspartoacylase-deficient tremor rat. *Neurochem. Res.* **34**, 138–148 (2009).
34. M. H. Baslow, Functions of *N*-acetyl-L-aspartate and *N*-acetyl-L-aspartylglutamate in the vertebrate brain: Role in glial cell-specific signaling. *J. Neurochem.* **75**, 453–459 (2000).
35. M. H. Baslow, D. N. Guilfoyle, Are astrocytes the missing link between lack of brain aspartoacylase activity and the spongiform leukodystrophy in Canavan disease? *Neurochem. Res.* **34**, 1523–1534 (2009).
36. O. Sacks, W. J. Brown, M. J. Aguilar, Spongy degeneration of white matter: Canavan's sclerosis. *Neurology* **15**, 165–171 (1965).
37. P. Gambetti, W. J. Mellman, N. K. Gonatas, Familial spongy degeneration of the central nervous system (Van Bogaert-Bertrand disease). An ultrastructural study. *Acta Neuropathol.* **12**, 103–115 (1969).
38. B. T. Adornato, J. S. O'Brien, P. W. Lampert, T. F. Roe, H. B. Neustein, Cerebral spongy degeneration of infancy. A biochemical and ultrastructural study of affected twins. *Neurology* **22**, 202–210 (1972).
39. S. G. Waxman, J. D. Kocsis, P. K. Stys, *The Axon* (Oxford Univ Press, New York, 1995), pp. 422–423.
40. M. Adachi, L. Schneck, J. Cara, B. W. Volk, Spongy degeneration of the central nervous system (van Bogaert and Bertrand type; Canavan's disease). A review. *Hum. Pathol.* **4**, 331–347 (1973).
41. H. D. Yan, K. Ishihara, T. Serikawa, M. Sasa, Activation by *N*-acetyl-L-aspartate of acutely dissociated hippocampal neurons in rats via metabotropic glutamate receptors. *Epilepsia* **44**, 1153–1159 (2003).
42. K. Kitada, T. Akimitsu, Y. Shigematsu, A. Kondo, T. Maihara, N. Yokoi, T. Kuramoto, M. Sasa, T. Serikawa, Accumulation of *N*-acetyl-L-aspartate in the brain of the Tremor rat, a mutant exhibiting absence-like seizure and spongiform degeneration in the central nervous system. *J. Neurochem.* **74**, 2512–2519 (2000).
43. E. C. Traeger, I. Rapin, The clinical course of Canavan disease. *Pediatr. Neurol.* **18**, 207–212 (1998).
44. B. J. Zeng, Z. H. Wang, L. A. Ribeiro, P. Leone, R. De Gasperi, S. J. Kim, S. Raghavan, E. Ong, G. M. Pastores, E. H. Kolodny, Identification and characterization of novel mutations of the aspartoacylase gene in non-Jewish patients with Canavan disease. *J. Inherit. Metab. Dis.* **25**, 557–570 (2002).
45. N. Zelnik, A. S. Luder, O. N. Elpeleg, V. Gross-Tsur, N. Amir, J. A. Hemli, A. Fattal, S. Harel, Protracted clinical course for patients with Canavan disease. *Dev. Med. Child Neurol.* **35**, 355–358 (1993).
46. P. Leone, C. G. Janson, S. J. McPhee, M. J. During, Global CNS gene transfer for a childhood neurogenetic enzyme deficiency: Canavan disease. *Curr. Opin. Mol. Ther.* **1**, 487–492 (1999).
47. P. Leone, C. G. Janson, L. Bilaniuk, Z. Wang, F. Sorgi, L. Huang, R. Matalon, R. Kaul, Z. Zeng, A. Freese, S. W. McPhee, E. Mee, M. J. During, Aspartoacylase gene transfer to the mammalian central nervous system with therapeutic implications for Canavan disease. *Ann. Neurol.* **48**, 27–38 (2000).
48. C. Janson, S. McPhee, L. Bilaniuk, J. Haselgrove, M. Testaiuti, A. Freese, D. J. Wang, D. Shera, P. Hurh, J. Rupin, E. Saslow, O. Goldfarb, M. Goldberg, G. Larijani, W. Sharrar, L. Liouterman, A. Camp, E. Kolodny, J. Samulski, P. Leone, Clinical protocol. Gene therapy of Canavan disease: AAV-2 vector for neurosurgical delivery of aspartoacylase gene (ASPA) to the human brain. *Hum. Gene Ther.* **13**, 1391–1412 (2002).
49. R. Matalon, S. Surendran, P. L. Rady, M. J. Quast, G. A. Campbell, K. M. Matalon, S. K. Tyring, J. Wei, C. S. Peden, E. L. Ezell, N. Muzyczka, R. J. Mandel, Adeno-associated virus-mediated aspartoacylase gene transfer to the brain of knockout mouse for Canavan disease. *Mol. Ther.* **7**, 580–587 (2003).
50. S. W. McPhee, J. Francis, C. G. Janson, T. Serikawa, K. Hyland, E. O. Ong, S. S. Raghavan, A. Freese, P. Leone, Effects of AAV-2-mediated aspartoacylase gene transfer in the tremor rat model of Canavan disease. *Brain Res. Mol. Brain Res.* **135**, 112–121 (2005).
51. B. J. Zeng, G. M. Pastores, P. Leone, S. Raghavan, Z. H. Wang, L. A. Ribero, P. Torres, E. Ong, E. H. Kolodny, Mutation analysis of the aspartoacylase gene in non-Jewish patients with Canavan disease. *Adv. Exp. Med. Biol.* **576**, 165–173; discussion 361-363 (2006).
52. C. G. Janson, E. H. Kolodny, B. J. Zeng, S. Raghavan, G. Pastores, P. Torres, M. Assadi, S. McPhee, O. Goldfarb, B. Saslow, A. Freese, D. J. Wang, L. Bilaniuk, D. Shera, P. Leone, Mild-onset presentation of Canavan's disease associated with novel G212A point mutation in aspartoacylase gene. *Ann. Neurol.* **59**, 428–431 (2006).
53. S. M. Haley, *Pediatric Evaluation of Disability Index (PEDI). Development, Standardization, and Administration Manual* (Center for Rehabilitation Effectiveness, Boston, MA, 1998).
54. N. M. Laird, J. H. Ware, Random-effects models for longitudinal data. *Biometrics* **38**, 963–974 (1982).
55. C. G. Janson, M. Assadi, J. Francis, L. Bilaniuk, D. Shera, P. Leone, Lithium citrate for Canavan disease. *Pediatr. Neurol.* **33**, 235–243 (2005).
56. W. S. Cleveland, Robust locally weighted regression and smoothing scatterplots. *J. Am. Stat. Assoc.* **74**, 829–836 (1979).
57. D. Russell, *The Gross Motor Function Measure Manual* (CanChild Centre for Childhood Disability Research, McMaster University, Hamilton, Canada, 1993).
58. E. M. Mullen, *The Mullen Scales of Early Learning* (American Guidance Service, Circle Pines, MN, 1995).
59. S. W. McPhee, C. G. Janson, C. Li, R. J. Samulski, A. S. Camp, J. Francis, D. Shera, L. Liouterman, M. Feely, A. Freese, P. Leone, Immune responses to AAV in a phase I study for Canavan disease. *J. Gene Med.* **8**, 577–588 (2006).
60. W. W. Lam, Z. J. Wang, H. Zhao, G. T. Berry, P. Kaplan, J. Gibson, B. S. Kaplan, L. T. Bilaniuk, J. V. Hunter, J. C. Haselgrove, R. A. Zimmerman, ^{1}H MR spectroscopy of the basal ganglia in childhood: A semiquantitative analysis. *Neuroradiology* **40**, 315–323 (1998).
61. A. Horská, W. E. Kaufman, L. J. Brant, S. Naidu, J. C. Harris, P. B. Barker, In vivo quantitative proton MRSI study of brain development from childhood to adolescence. *J. Magn. Reson. Imaging* **15**, 137–143 (2002).
62. R. Kreis, T. Ernst, B. D. Ross, Development of the human brain: In vivo quantification of metabolite and water content with proton magnetic resonance spectroscopy. *Magn. Reson. Med.* **30**, 424–437 (1993).
63. R. Xu, C. G. Janson, M. Mastakov, P. Lawlor, D. Young, A. Mouravlev, H. Fitzsimmons, K. L. Choi, H. Ma, M. Dragunow, P. Leone, Q. Chen, B. Dicker, M. J. During, Quantitative comparison of expression with adeno-associated virus (AAV-2) brain-specific gene cassettes. *Gene Ther.* **8**, 1323–1332 (2001).

64. B. F. Kirmani, D. M. Jacobowitz, A. T. Kallarakal, M. A. Namboodiri, Aspartoacylase is restricted primarily to myelin synthesizing cells in the CNS: Therapeutic implications for Canavan disease. *Brain Res. Mol. Brain Res.* **107**, 176–182 (2002).
65. M. Chopra, Y. Yao, T. J. Blake, D. R. Hampson, E. C. Johnson, The neuroactive peptide *N*-acetylaspartylglutamate is not an agonist at the metabotropic glutamate receptor subtype 3 of metabotropic glutamate receptor. *J. Pharmacol. Exp. Ther.* **330**, 212–219 (2009).
66. G. L. Westbrook, M. L. Mayer, M. A. Namboodiri, J. H. Neale, High concentrations of *N*-acetylaspartylglutamate (NAAG) selectively activate NMDA receptors on mouse spinal cord neurons in cell culture. *J. Neurosci.* **6**, 3385–3392 (1986).
67. Y. Rubin, M. C. LaPlaca, D. H. Smith, L. E. Thibault, R. E. Lenkinski, The effect of *N*-acetylaspartate on the intracellular free calcium concentration in NTera2-neurons. *Neurosci. Lett.* **198**, 209–212 (1995).
68. T. Akimitsu, K. Kurisu, R. Hanaya, K. Iida, Y. Kiura, K. Arita, H. Matsubayashi, K. Ishihara, K. Kitada, T. Serikawa, M. Sasa, Epileptic seizures induced by *N*-acetyl-L-aspartate in rats: In vivo and in vitro studies. *Brain Res.* **861**, 143–150 (2000).
69. M. Klugmann, C. B. Leichtlein, C. W. Symes, T. Serikawa, D. Young, M. J. During, Restoration of aspartoacylase activity in CNS neurons does not ameliorate motor deficits and demyelination in a model of Canavan disease. *Mol. Ther.* **11**, 745–753 (2005).
70. E. Martin, A. Capone, J. Schneider, J. Hennig, T. Thiel, Absence of *N*-acetylaspartate in the human brain: Impact on neurospectroscopy? *Ann. Neurol.* **49**, 518–521 (2001).
71. S. Kamoshita, I. Rapin, K. Suzuki, K. Suzuki, Spongy degeneration of the brain. A chemical study of two cases including isolation and characterization of myelin. *Neurology* **18**, 975–985 (1968).
72. J. S. Francis, L. Strande, V. Markov, P. Leone, Aspartoacylase supports oxidative energy metabolism during myelination. *J. Cereb. Blood Flow Metab.* **32**, 1725–1736 (2012).
73. R. Segel, Y. Anikster, S. Zevin, A. Steinberg, W. A. Gahl, D. Fisher, O. Staretz-Chacham, A. Zimran, G. Altarescu, A safety trial of high dose glyceryl triacetate for Canavan disease. *Mol. Genet. Metab.* **103**, 203–206 (2011).
74. M. L. Escolar, M. D. Poe, J. M. Provenzale, K. C. Richards, J. Allison, S. Wood, D. A. Wenger, D. Pietryga, D. Wall, M. Champagne, R. Morse, W. Krivit, J. Kurtzberg, Transplantation of umbilical-cord blood in babies with infantile Krabbe's disease. *N. Engl. J. Med.* **352**, 2069–2081 (2005).
75. S. L. Staba, M. L. Escolar, M. Poe, Y. Kim, P. L. Martin, P. Szabolcs, J. Allison-Thacker, S. Wood, D. A. Wenger, P. Rubinstein, J. J. Hopwood, W. Krivit, J. Kurtzberg, Cord-blood transplants from unrelated donors in patients with Hurler's syndrome. *N. Engl. J. Med.* **350**, 1960–1969 (2004).

Acknowledgments: We thank M. Feely and A. Turtz for neurosurgical care; S. DaSilva for pediatric intensive care; E. Saslow for psychometric assessments; H. Fitzsimmons and T. Lawlor of the University of Auckland and A. Camp of UNC Clinical Vector Core for AAV vector production; and G. Spinella and D. Tagle for helpful input on the clinical protocol. The study protocol was publicly reviewed by the Recombinant DNA Advisory Committee, NIH Office of Rare Diseases, and the FDA. **Funding:** Supported by NINDS RO1-NS42120 and additional funding from the Canavan Research Foundation, Canavan Research Illinois, Jacob's Cure, the National Endowment for Alzheimer's Research, and the Ralph and Lois Silver Foundation. **Author contributions:** P.L. and C.G.J. were primarily responsible for experimental design, data analysis, and writing of this paper. D.S., S.W.J.M., and J.S.F. were responsible for multivariate data analyses. L.T.B. and D.-J.W. were responsible for collection and interpretation of MRI data. E.H.K. was responsible for *ASPA* mutational analyses. M.J.D., D.Y., and R.J.S. directed clinical grade AAV-*ASPA* production. O.G., M.A., H.W.G., and A.F. were involved with implementation of the clinical protocol. **Competing interests:** R.J.S. holds patents on AAV vector production and applications (US5139941 "AAV Transduction Vectors"; US6458587 "Helper-Virus Free AAV Production"). The other authors declare that they have no competing interests.

Submitted 14 November 2011
Accepted 30 November 2012
Published 19 December 2012
10.1126/scitranslmed.3003454

Citation: P. Leone, D. Shera, S. W.J. McPhee, J. S. Francis, E. H. Kolodny, L. T. Bilaniuk, D.-J. Wang, M. Assadi, O. Goldfarb, H. W. Goldman, A. Freese, D. Young, M. J. During, R. J. Samulski, C. G. Janson, Long-term follow-up after gene therapy for Canavan disease. *Sci. Transl. Med.* **4**, 165ra163 (2012).

www.sciencetranslationalmedicine.org/cgi/content/full/4/165/165ra163/DC1

Supplementary Materials for

Long-Term Follow-Up After Gene Therapy for Canavan Disease

Paola Leone,* David Shera, Scott W.J. McPhee, Jeremy S. Francis, Edwin H. Kolodny, Larissa T. Bilaniuk, Dah-Jyuu Wang, Mitra Assadi, Olga Goldfarb, H. Warren Goldman, Andrew Freese, Deborah Young, Matthew J. During, R. Jude Samulski, Christopher G. Janson

*To whom correspondence should be addressed. E-mail: leonepa@umdnj.edu

Published 19 December 2012, *Sci. Transl. Med.* **4**, 165ra163 (2012)
DOI: 10.1126/scitranslmed.3003454

The PDF file includes:

Table S1. Demographics of the natural history subjects.

Subjects who were not selected for gene therapy in one of the three treatment groups were followed with MRI/MRS as part of a natural history study which examined levels of brain NAA. Untreated subjects were followed longitudinally and quantitative clinical testing and NAA levels were included in modeling data for pre-/post-treatment comparisons. Age is shown in months at time of enrollment. The selection and enrollment of subjects was previously described in our clinical protocol (Janson *et al.,* 2002). This table demonstrates the range of mutations as well as the age and sex distribution of untreated subjects. Data from untreated subjects and untreated subjects who went on to receive gene therapy were treated as equivalent, based on the fact that all the common gene mutations have been shown to be biochemically equivalent. There are certain very rare exceptions of mild genotypes such as G212A (Janson *et al.,* 2005), but these were excluded from this study.

SUBJECT I.D.	SEX	AGE	ASPA MUTATIONS
01-118-11	M	19	914C→A (A305E)
			47T→C (I16T)
01-118-16	M	29	244-245 del AT (codon 82 del)
			244-245 del AT (codon 82 del)
01-118-17	F	16	914C→A (A305E)
			815G→C (L272P)
01-118-18	M	41	502C→T (R168C)
			exon 2 deletion
01-118-21	M	5	914C→A (A305E)
			362A→T (N121I)
01-118-22	M	7	914C→A (A305E)
			914C→A (A305E)
01-118-23	M	9	733A→G (H244L)
			733A→G (H244L)
01-118-25	M	20	914C→A (A305E)
			640G→T (G214X)
01-118-26	M	8	854A→C (E285A)
			854A→C (E285A)
01-118-20	M	8	854A→C (E285A)
			854A→C (E285A)
01-118-19	M	10	914C→A (A305E)
			914C→A (A305E)
01-118-10	M	7	914C→A (A305E)
			UNK
01-118-14	M	41	854A→C (E285A)
			854A→C (E285A)
01-118-06	M	10	41T→G (V14G)
			541A→C (P181T)
01-118-13	F	16	914C→A (A305E)
			914C→A (A305E)

Table S2. Other metabolites from ^{1}H-MRS.

1. Choline ^{1}H·MRS

Choline-containing compounds (e.g.. phosphatidylcholine) are known to be important in myelination, and mean choline concentrations usually decrease from 2.6 mM in neonates to less than 2.2 mM during the first year of life, presumably during myelin incorporation, with a normal adult range of 0.8-1.4 mM. In patients with untreated Canavan disease, the mean choline peak was abnormally low compared to age-matched concentrations in subjects without Canavan disease, with negative slopes in the basal ganglia, periventricular, and frontal regions. We observed a small but statistically significant post-treatment increase in mean choline concentrations in conjunction with a more negative slope, which could represent increased utilization of choline. However, average choline concentrations remained < 1 mM before and after treatment.

2. Creatine ^{1}H·MRS

Creatine is important for cellular energetics, particularly in the form of phosphocreatine in astrocytes. Normal brain values are usually stable in post-natal life and are in the range of 5-7 mM. We previously reported lower concentrations in untreated Canavan disease patients in the range of 2-6 mM, with a negative slope in the periventricular and frontal regions. In the current study, there was a small but statistically significant post-treatment decrease in slope of creatine in the periventricular region, in conjunction with a small increase in mean creatine concentrations in all regions, which did not reach statistical significance.

3. Myoinositol ^{1}H·MRS

The most prominent peak of the newborn 'H·MRS is myoinositol, which decreases during myelination in the postnatal period. Found primarily in astrocytes, myoinositol has multiple roles as osmolyte, precursor for lipid synthesis, and in phosphoinositol intracellular signaling. and may be either elevated or decreased in various disease states. Normal mean myoinositol concentrations are approximately 12 mM at birth, 3.5-8 mM in infants, and slightly lower in adults. Prior studies found elevated myoinositol concentrations in Canavan disease. The current study indicates that untreated myoinositol concentrations In the 0-2 year age range are 4.0 mM (S.D +/- 1.1), and the slope and mean concentrations of myoinositol did not change post-treatment.

4. Validation of Brain ^{1}H·MRS with Serum and Urine NAA

Under ordinary conditions NAA is found only in the brain, but in Canavan disease excess intracerebral NAA is extruded, leading to NAA acidemia and aciduria, a process which is still poorly understood. After immunological analyses were completed, limited serum samples remained for NAA biochemical analysis, typically only three observations, but these were analyzed by HPLC in order to validate results obtained by other methods such as 'H-MRS. These data were intended as a control for ^{1}H-MRS results. NAA is normally undetectable in serum, and can be quite variable in Canavan disease. In the most widely cited paper, Matalon (1988) reported mean plasma NAA of approximately 1000μM and urine NAA of 2.2mM (normalized to creatinine), but it should be noted that those values were based upon single, static measurements from only three patients. Hagenfeldt (1987) had reported 100-fold lower blood NAA based on measurements from two patients, which is more similar to our measurements. We observed an approximately 50% post-treatment drop in mean blood levels of NAA from 27 to 13μM, consistent with the observed drop in brain NAA using spectroscopic methods. We also measured urine NAA levels before and after treatment and found an approximate 20% drop in mean levels, from 1.75 to 1.51 mmol NAA/mmol creatinine. Formal statistical analysis of urine and serum specimens was complicated by limited samples. Even more limited data were available for NAA levels from cerebrospinal fluid, which was sampled from several subjects with pre-implanted Ommaya reservoirs. The pretreatment and perioperative values were approximately 0.3mM, similar to levels previously reported, but post-treatment values were not able to be collected.

These tables show the changes in metabolites other than NAA. The top table in each section shows slopes with pre/post comparison, the middle shows levels with pre/post comparison, and the bottom shows levels with pre/ post comparison using at-test rather than the generalized linear model.

Choline, Table of Coefficients & Contrasts (GLMM)

	Pre-treatment		Post-treatment		Post vs. Pre	
	coefficient	p-value	coefficient	p-value	coefficient	p-value
Frontal	-0.003	0.136	-0.015	0.001	-0.011	0.018
Periventricular	0.00001	0.995	-0.011	0.012	-0.011	0.022
Occipital	-0.002	0.397	-0.012	0.006	-0.010	0.031
Basal ganglia	-0.001	0.923	-0.015	<0.0006	-0.015	0.002

Choline, Table of Level Estimates & Contrasts (GLMM)

	Pre-treatment	Post-treatment	Post vs. Pre	
	coefficient	coefficient	difference	p-value
Frontal	0.614	0.756	+0.143	0.020
Periventricular	0.448	0.494	+0.046	0.452
Occipital	0.436	0.537	+0.131	0.033
Basal ganglia	0.552	0.731	+0.179	0.003

Choline, Table of Level Estimates & Contrasts (Mean & S.D. with T-tests)

	Pre-treatment		Post-treatment		Post vs. Pre	
	mean	S.D	mean	S.D	difference	p-value
Frontal	0.550	0.308	0.627	0.244	+0.077	0.100
Periventricular	0.474	0.261	0.534	0.218	+0.060	0.138
Occipital	0.418	0.239	0.539	0.175	+0.121	0.0007
Basal ganglia	0.583	0.281	0.721	0.280	+0.138	0.003

Creatine, Table of Coefficients & Contrasts (GLMM)

	Pre-treatment		Post-treatment		Post vs. Pre	
	coefficient	p-value	coefficient	p-value	coefficient	p-value
Frontal	0.008	0.955	-0.028	0.056	-0.036	0.047
Periventricular	0.015	0.074	-0.017	0.243	-0.032	0.076
Occipital	0.005	0.560	-0.013	0.350	-0.018	0.311
Basal ganglia	0.012	0.158	-0.019	0.185	-0.031	0.084

Creatine, Table of Level Estimates & Contrasts (GLMM)

	Pre-treatment	Post-treatment	Post vs. Pre	
	coefficient	coefficient	difference	p-value
Frontal	2.34	2.70	+0.360	0.214
Periventricular	2.07	1.90	-0.172	0.552
Occipital	3.19	3.27	+0.080	0.780
Basal ganglia	3.28	3.59	+0.298	0.302

Creatine, Table of Level Estimates & Contrasts (Mean & S.D. with T-tests)

	Pre-treatment		Post-treatment		Post vs. Pre	
	mean	S.D	mean	S.D	difference	p-value
Frontal	2.66	1.13	2.98	1.09	+0.320	0.081
Periventricular	2.59	1.12	2.67	0.937	+0.080	0.667
Occipital	3.43	1.45	3.66	0.813	+0.230	0.244
Basal ganglia	3.77	2.65	4.29	1.46	+0.520	0.048

Myoinositol, Table of Coefficients & Contrasts (GLMM)

	Pre-treatment		Post-treatment		Post vs. Pre	
	coefficient	p-value	coefficient	p-value	coefficient	p-value
Frontal	+0.013	0.432	-0.023	0.298	-0.035	0.237
Periventricular	+0.015	0.355	-.0300	0.175	-0.044	0.137
Occipital	-0.003	0.859	+0.008	0.723	+0.011	0.723
Basal ganglia	+0.005	0.758	-0.021	0.343	-0.026	0.390

Myoinositol, Table of Level Estimates & Contrasts (GLMM)

	Pre-treatment	Post-treatment	Post vs. Pre	
	coefficient	coefficient	difference	p-value
Frontal	4.05	3.87	-0.180	0.648
Periventricular	4.19	3.81	-0.375	0.341
Occipital	4.75	4.55	-0.199	0.612
Basal ganglia	4.52	4.83	+0.301	0.444

Myoinositol, Table of Level Estimates & Contrasts (Mean & S.D. with T-tests)

	Pre-treatment		Post-treatment		Post vs. Pre	
	mean	S.D	mean	S.D	difference	p-value
Frontal	4.42	2.11	4.30	1.20	-0.120	0.685
Periventricular	4.65	2.02	4.23	1.11	-0.420	0.129
Occipital	4.69	2.07	4.63	1.09	-0.060	0.839
Basal ganglia	4.72	2.33	4.82	1.52	+0.100	0.770

Table S3. Quantitative T1 Values by Region.

T1 and anisotropy were exploratory outcome measures and were intended solely for further hypothesis generating. Although data are reported here for completeness, the study was underpowered for T1 comparisons across multiple brain regions. Regional values are fully quantitative, but summary results are semi-quantitative (without Bonferroni correction) due to the small number of subjects vs. independent comparisons. The individual trends for changes in slope are shown below the table for the three regions discussed in the main text.

	Pre vs. Zero		Post vs. Zero		Post vs. Pre	
	Coefficient	p-value	Coefficient	p-value	Difference	p-value
Internal Capsule, L	-4.05	0.025	+1.94	0.371	5.99	0.031
Internal Capsule, R	-4.31	0.016	+1.51	0.459	5.83	0.024
Parietal WM, L	-4.54	0.008	-2.83	0.533	1.71	0.732
Parietal WM, R	-3.52	0.040	-0.81	0.854	2.72	0.580
Occipital WM, L	-2.74	0.135	0.64	0.900	3.38	0.531
Occipital WM, R	-4.17	0.029	-1.89	0.712	2.27	0.683
Frontal U-fibers, L	-4.88	0.0004	+2.36	0.532	7.24	0.068
Frontal U-fibers, R	-6.53	<.0001	+1.30	0.700	7.83	0.026
Pons, L	-5.48	0.0003	+4.49	0.223	9.97	0.014
Pons, R	-5.25	0.0004	+6.24	0.118	11.49	0.009
Midbrain, L	-5.55	0.0001	-2.33	0.494	3.22	0.377
Midbrain, R	-4.42	<.0001	+1.07	0.716	5.49	0.090
Putamen, L	-1.53	0.075	+0.860	0.269	2.39	0.062
Putamen, R	-2.28	<.0001	+0.570	0.476	2.85	0.002
Thalamus, L	-6.73	<.0001	-1.56	0.510	5.16	0.063
Thalamus, R	-7.24	<.0001	-1.81	0.478	5.43	0.071
Globus pallidus, L	-9.52	<.0001	-8.09	0.018	1.43	0.708
Globus pallidus, R	-6.58	0.0018	-5.06	0.104	1.51	0.698
Caudate, L	-3.28	<.0001	1.90	0.232	5.18	0.003
Caudate, R	-3.78	<.0001	-0.47	0.778	3.31	0.068
Splenium	**2.91**	**0.245**	**-5.44**	**0.063**	**-8.35**	**0.040**
Region Semiovale	**-0.64**	**0.799**	**-6.51**	**0.026**	**-5.87**	**0.149**
Parietal White Matter	**-3.07**	**0.221**	**-5.08**	**0.082**	**-2.02**	**0.620**

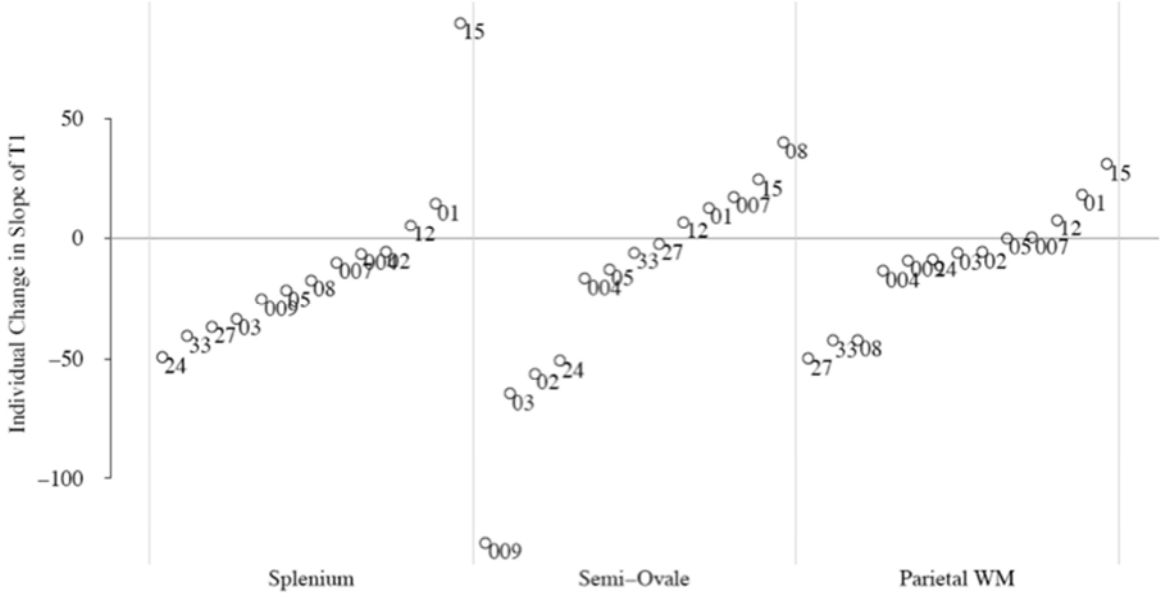

Fig. S1. Distribution of individual NAA individual values by region.

This graph shows the individual trends for post-treatment NAA slopes. The post-treatment trend in all 13 treated patients was a decrease in NAA slope in all regions. The most highly significant region was the periventricular region, but all regions showed decreased NAA levels after gene therapy. The frontal region showed a decrease in 11/13 patients and all other regions showed a decrease (negative slope) in 13/13 patients, but with somewhat wider variability among subjects. The least variable region was occipital, but this region also showed the smallest mean magnitude of change.

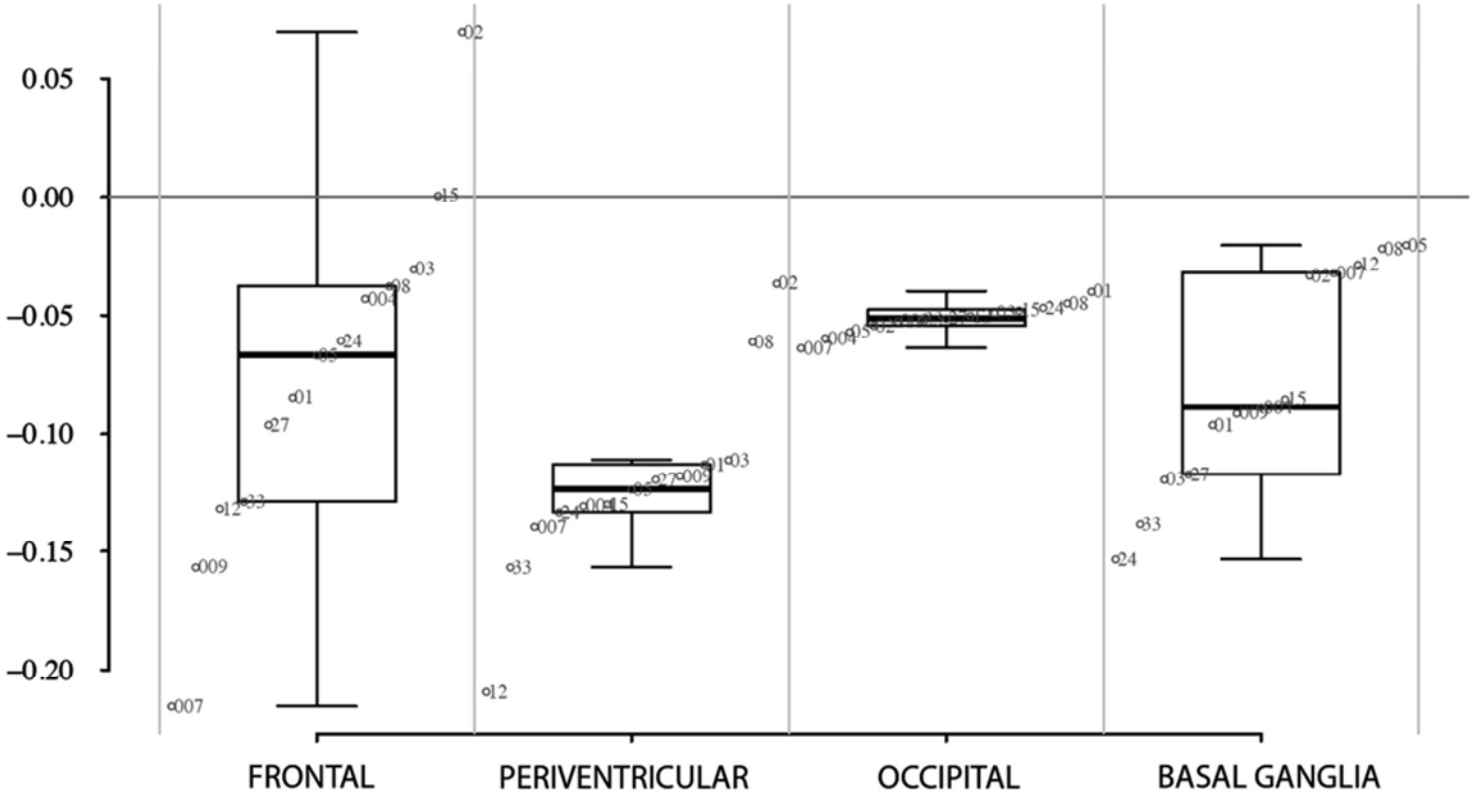

Fig. S2. Brain atrophy with LOESS scatterplot smoothing.

These four graphs show individual trends in brain atrophy for all subjects in the frontal (A), posterior (B), central (C), and cerebellar (D) regions, which are modeled using the "Loess" locally linear regression model, a nonparametric technique for describing bivariate relationships where the functional form is not known in advance. A "concave up" shape indicates a reversal in brain atrophy, while an increase in slope indicates a stabilization of gross atrophy. A negative slope indicates progressive gross brain atrophy. The broad line segments are pre-treatment, and the narrow extensions of the line segments are post-treatment. Some subjects such as the youngest subject 01-118-33 show a strong trend toward increasing brain mass, while others such as 01-118-01 had significant pre-treatment brain atrophy which improved in at least one region (i.e., posterior) but not in others.

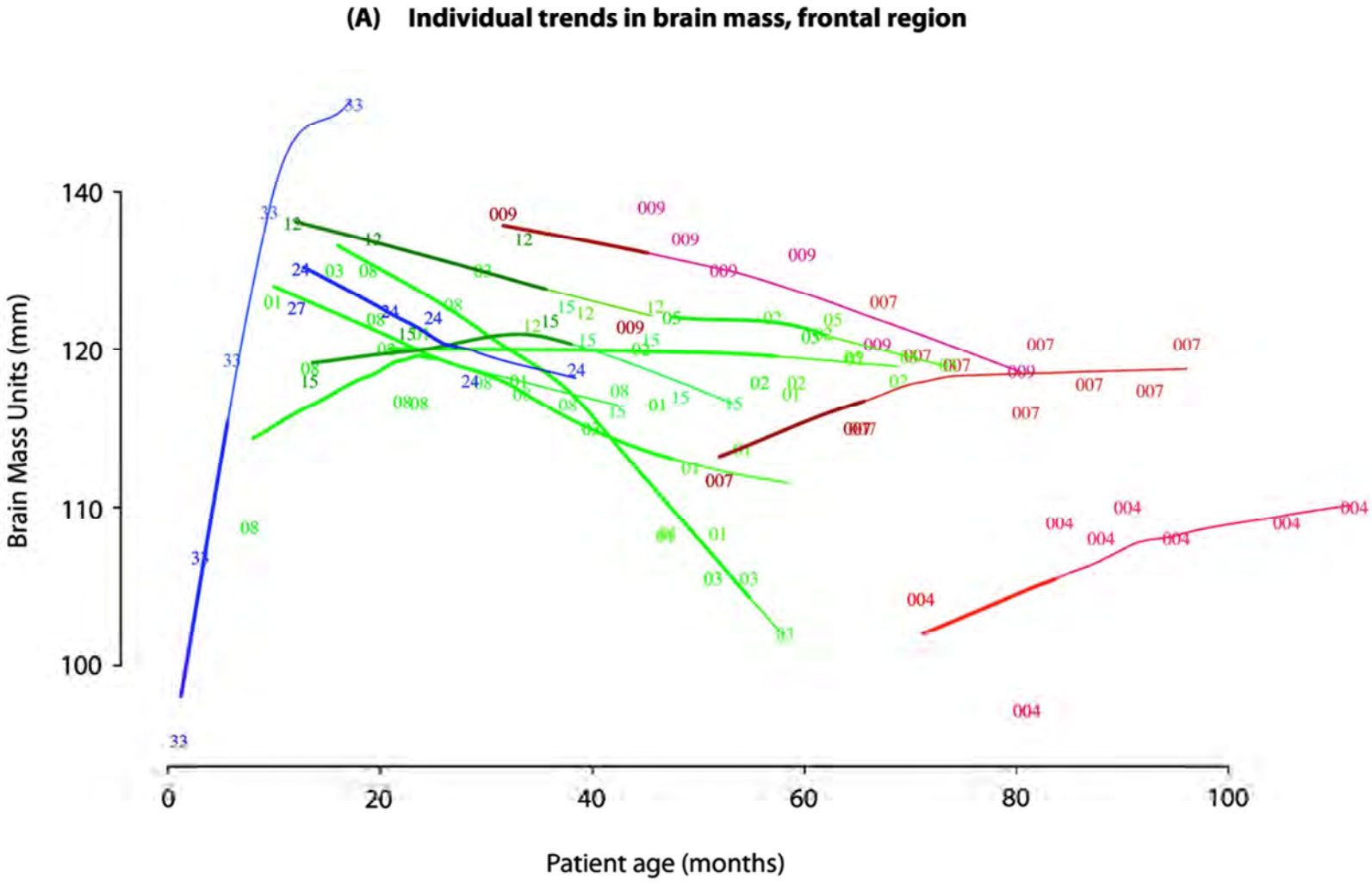

(B) Individual trends in brain mass, posterior region

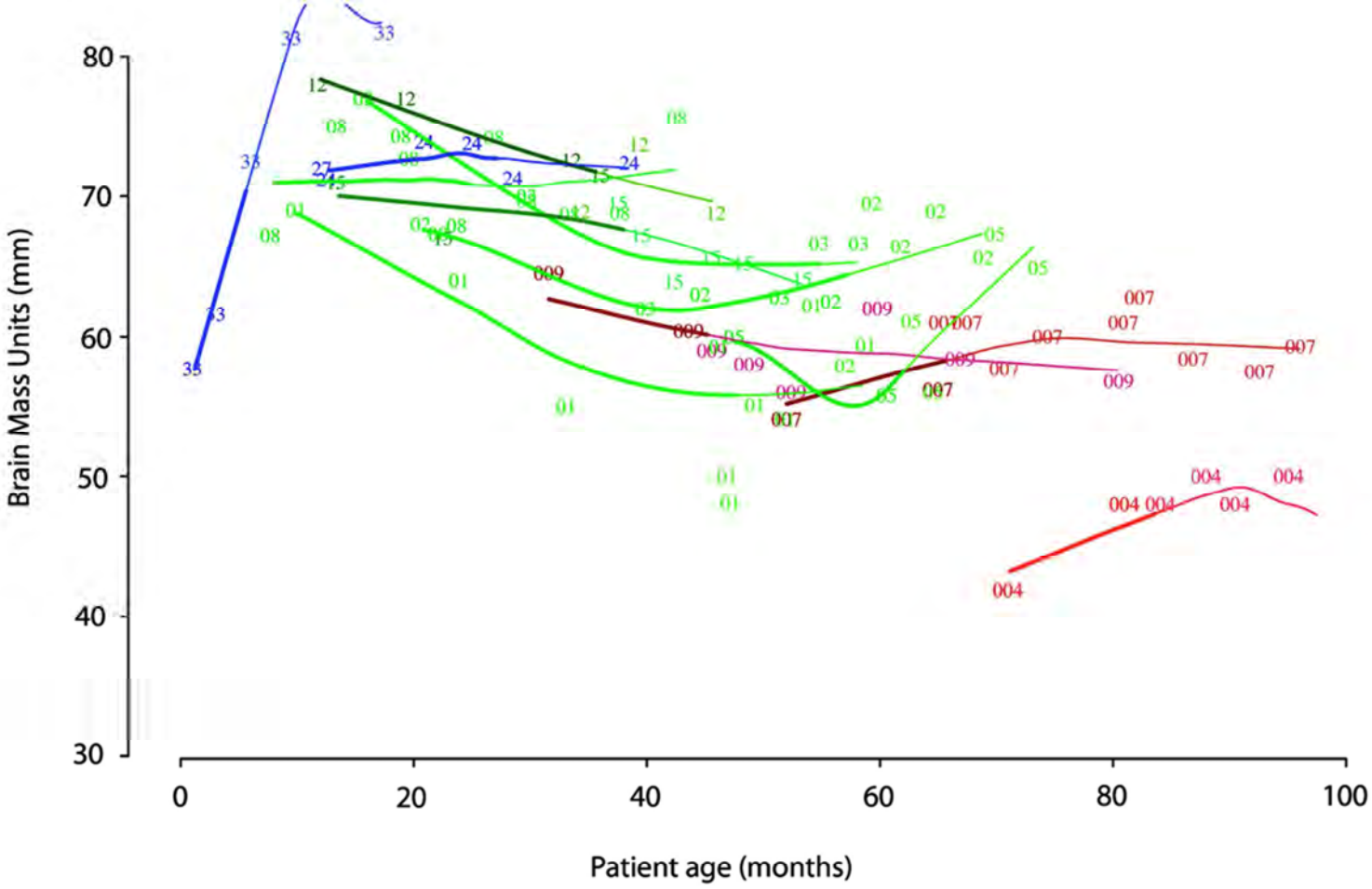

(C) Individual trends in brain mass, central region

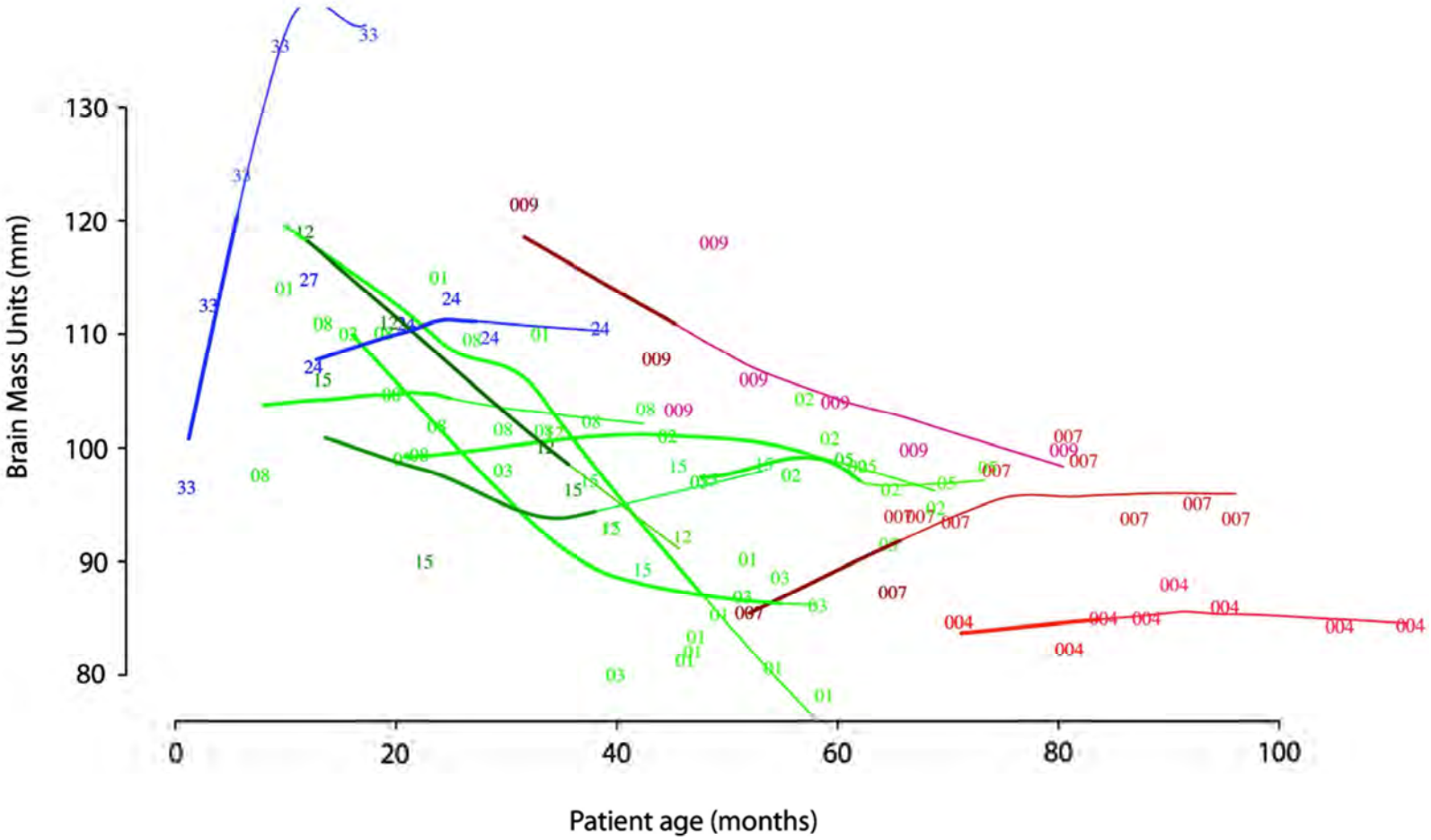

(D) Individual trends in brain mass, cerebellum

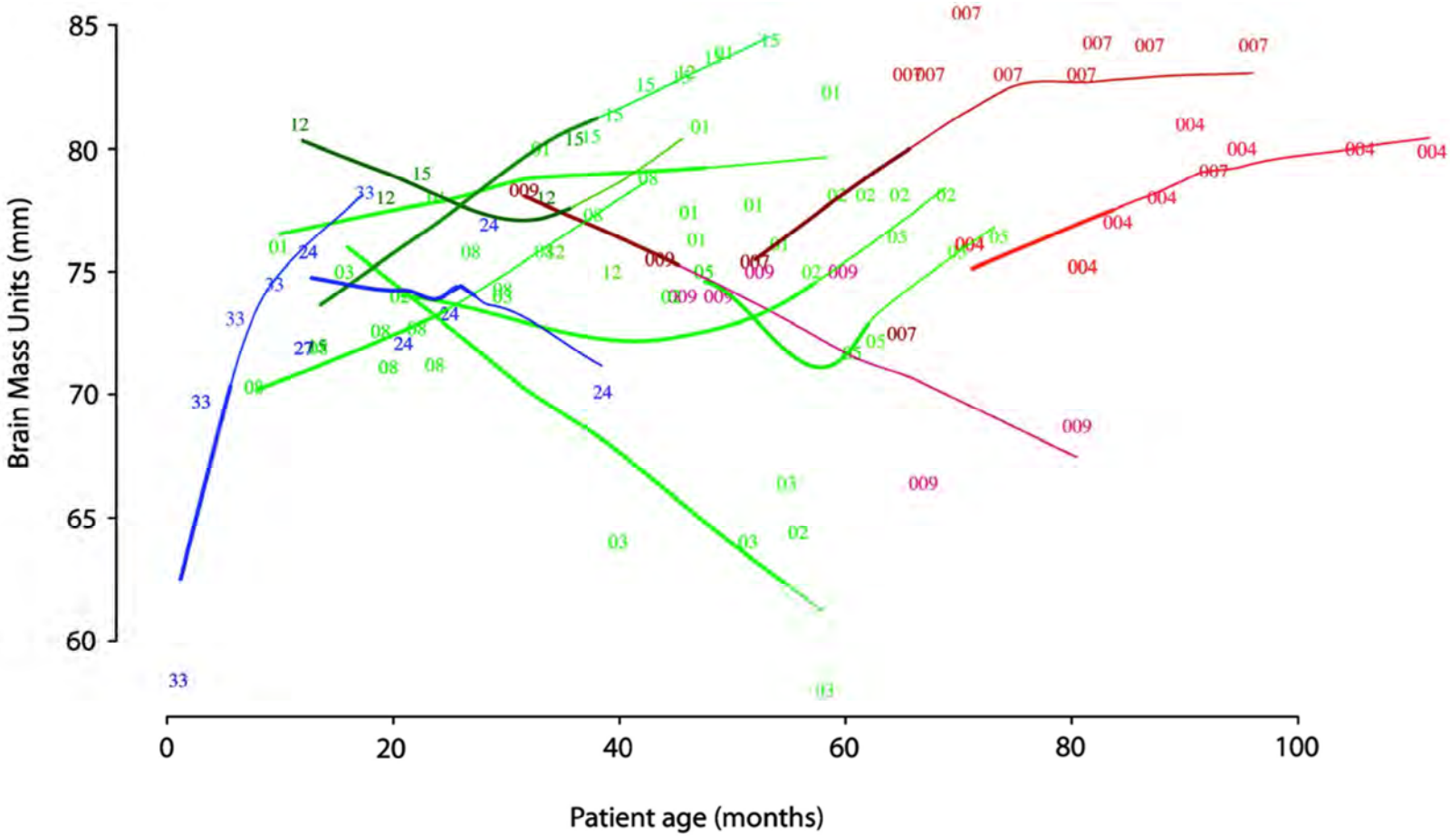

Fig. S3. Graph of pre-treatment vs. post-treatment GMFM.

This graph shows individual trajectories for the GMFM "lying and rolling" outcome, which was significant when the oldest subjects from the first treatment group (shown in red) were omitted. The mean magnitude of change in GMFM was variable among subjects. The youngest subject, shown in blue, had limited post-treatment values.

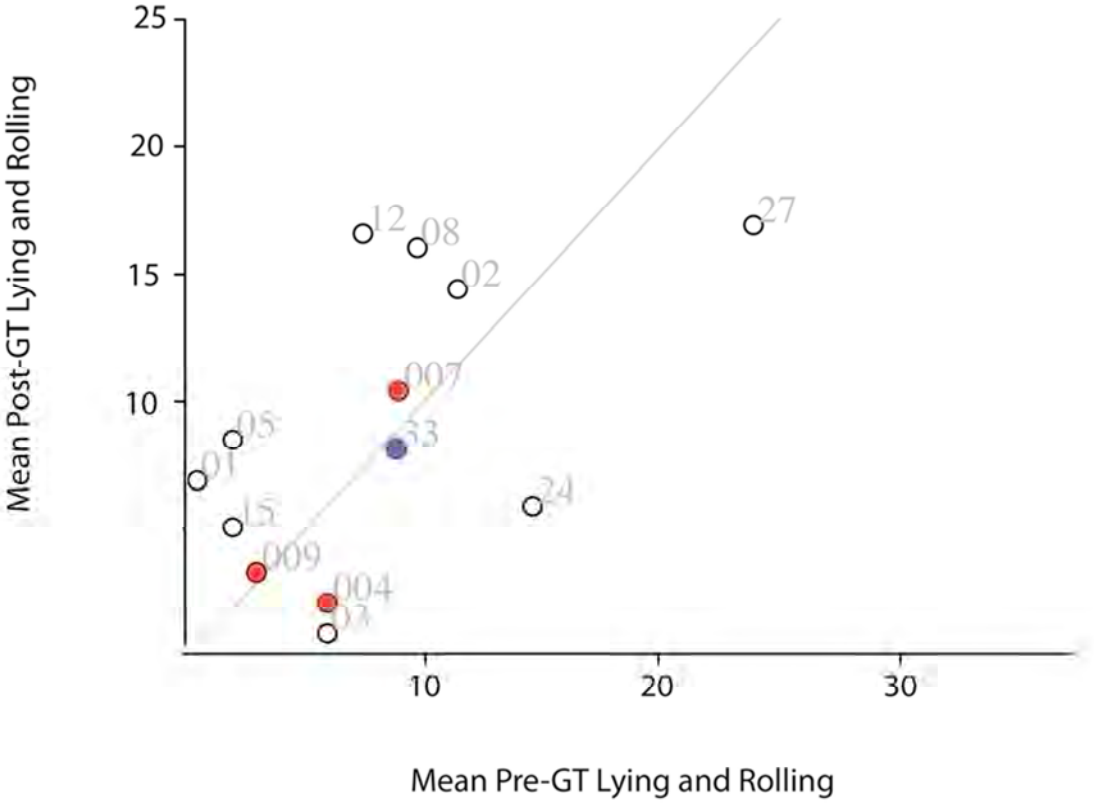

Fig. S4. Canavan alertness scale.

This graph plots the pre- and post-treatment values for alertness scale versus patient age and time from gene therapy. Alertness was part of the Canavan clinical exam which was performed by the study neurologist.

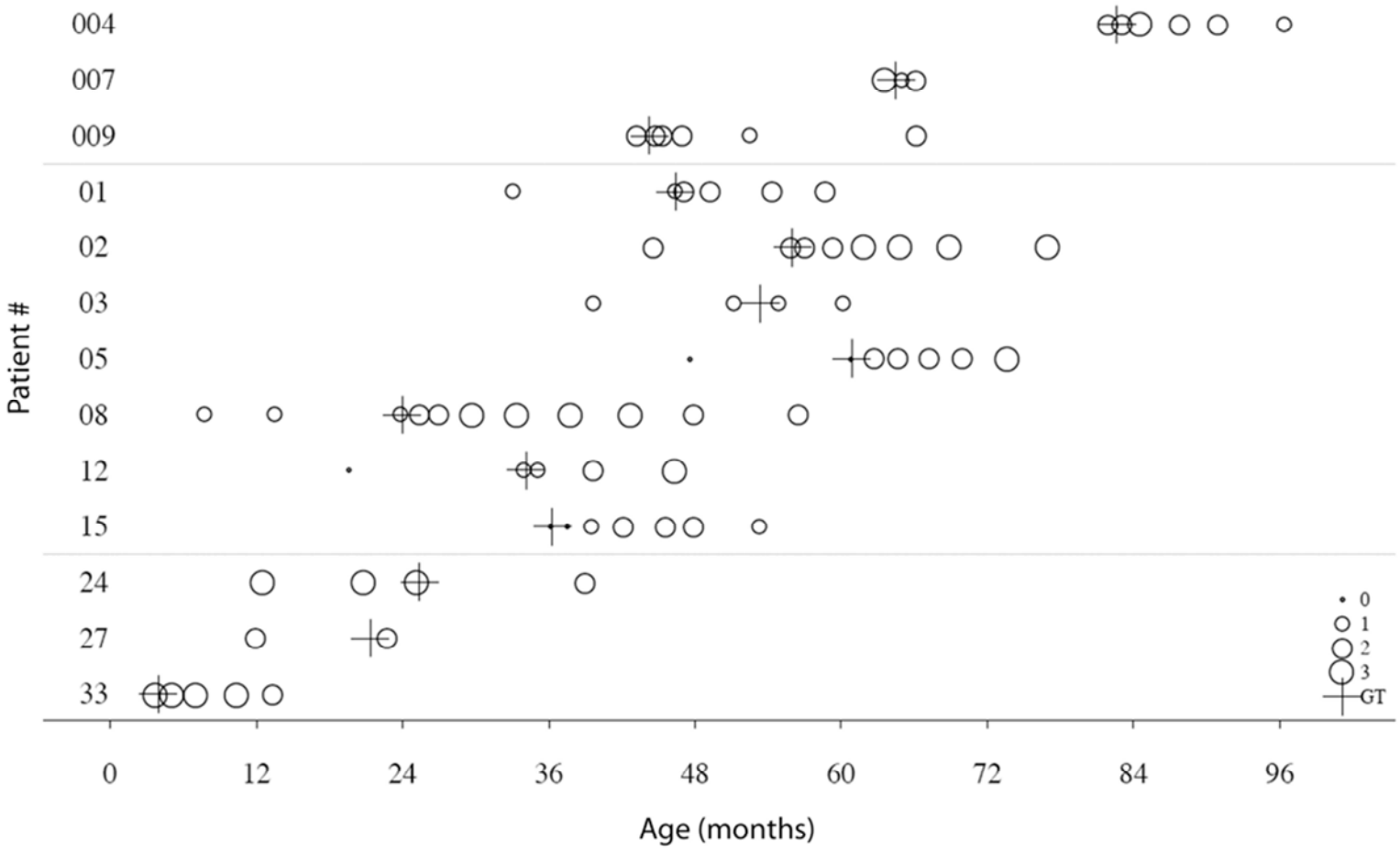

Fig. S5. Modified Ashworth scale of spasticity

This graph shows the summary data collected for the modified Ashworth spasticity scale, which was incorporated as part of the Canavan physical exam.

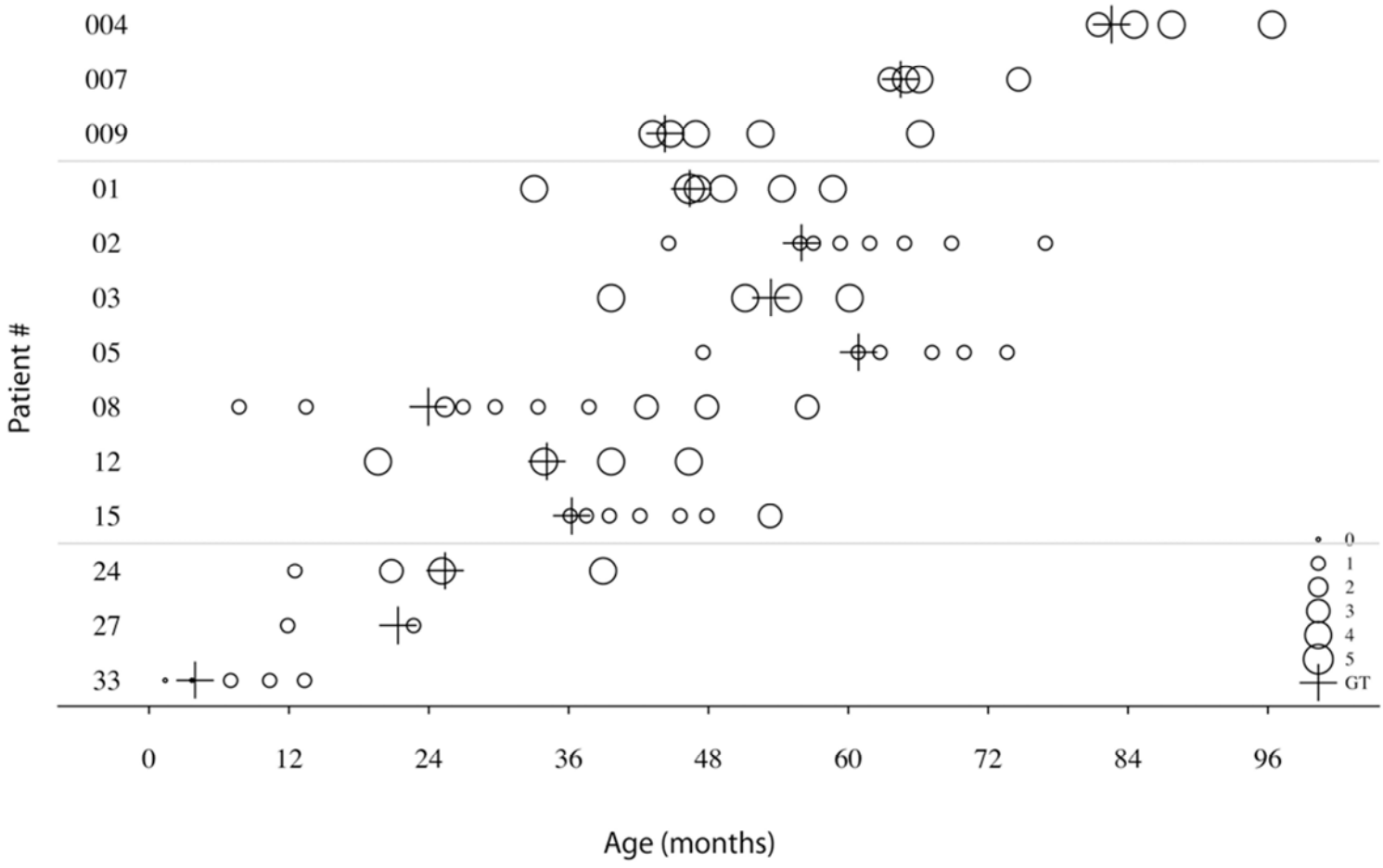

Fig. S6. PEDI social function, mean raw values plotted pre- vs. post-treatment.

Mean values on a per-patient basis for PEDI subscores through the 18 month time point, showing improvement or stable values in virtually all subjects.

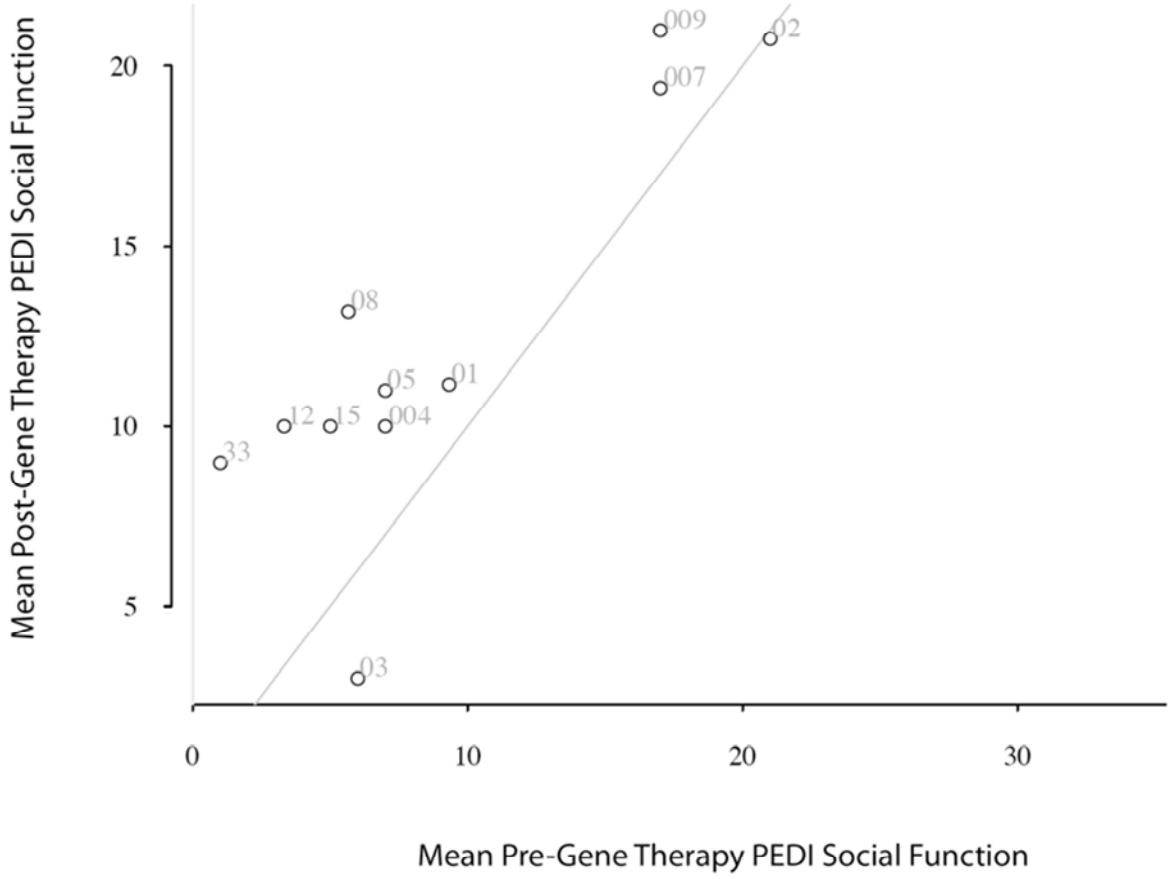

Fig. S7. Mullen expressive and receptive language.

Changes in expressive (top) and receptive (bottom) language shown for up to 24 months post-gene therapy. There were early but non-durable improvements in both subscores.

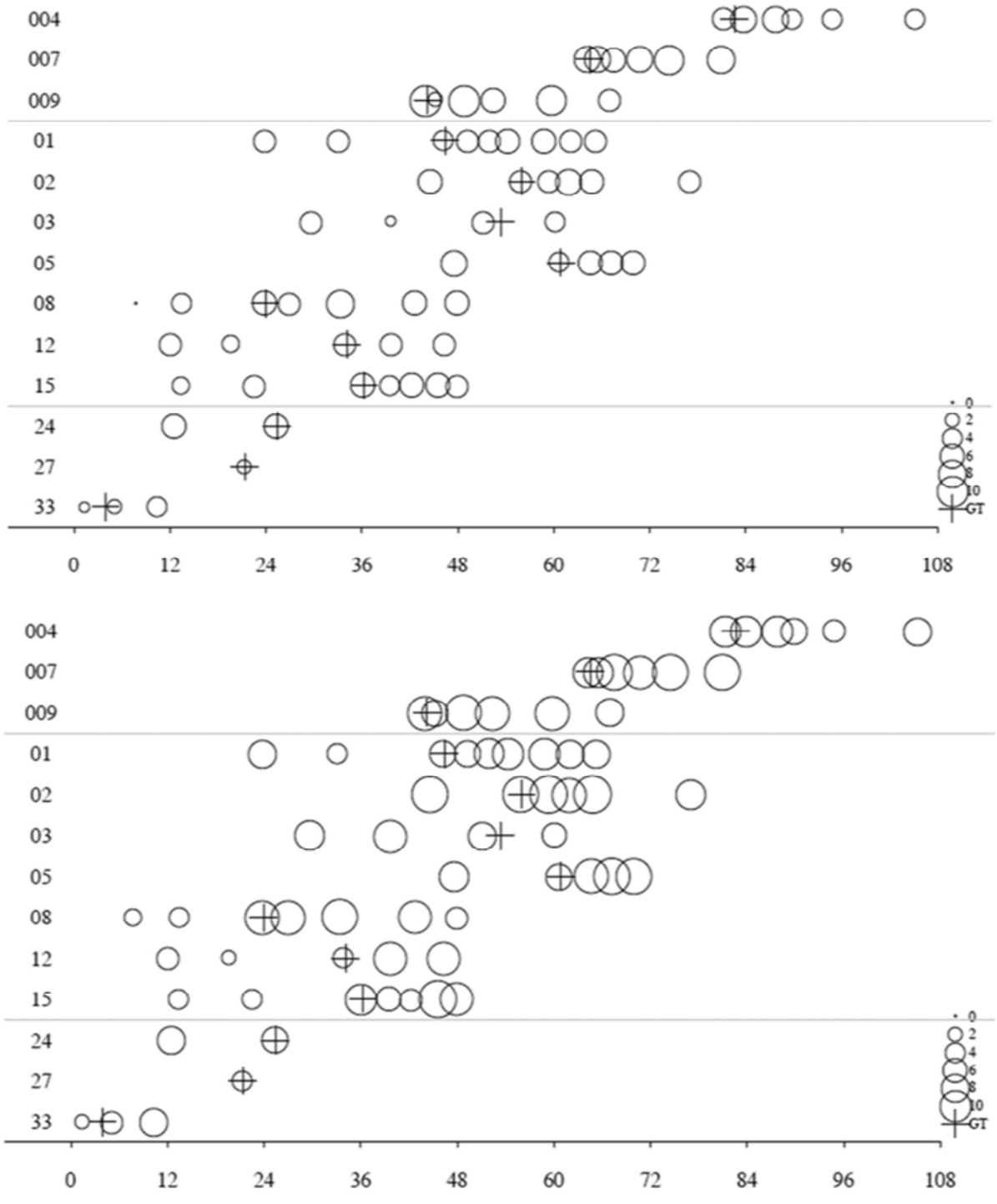

Fig. S8. Seizure frequency.
Seizure frequency shown pre- and post-gene therapy, for various seizure types on a per-subject basis.

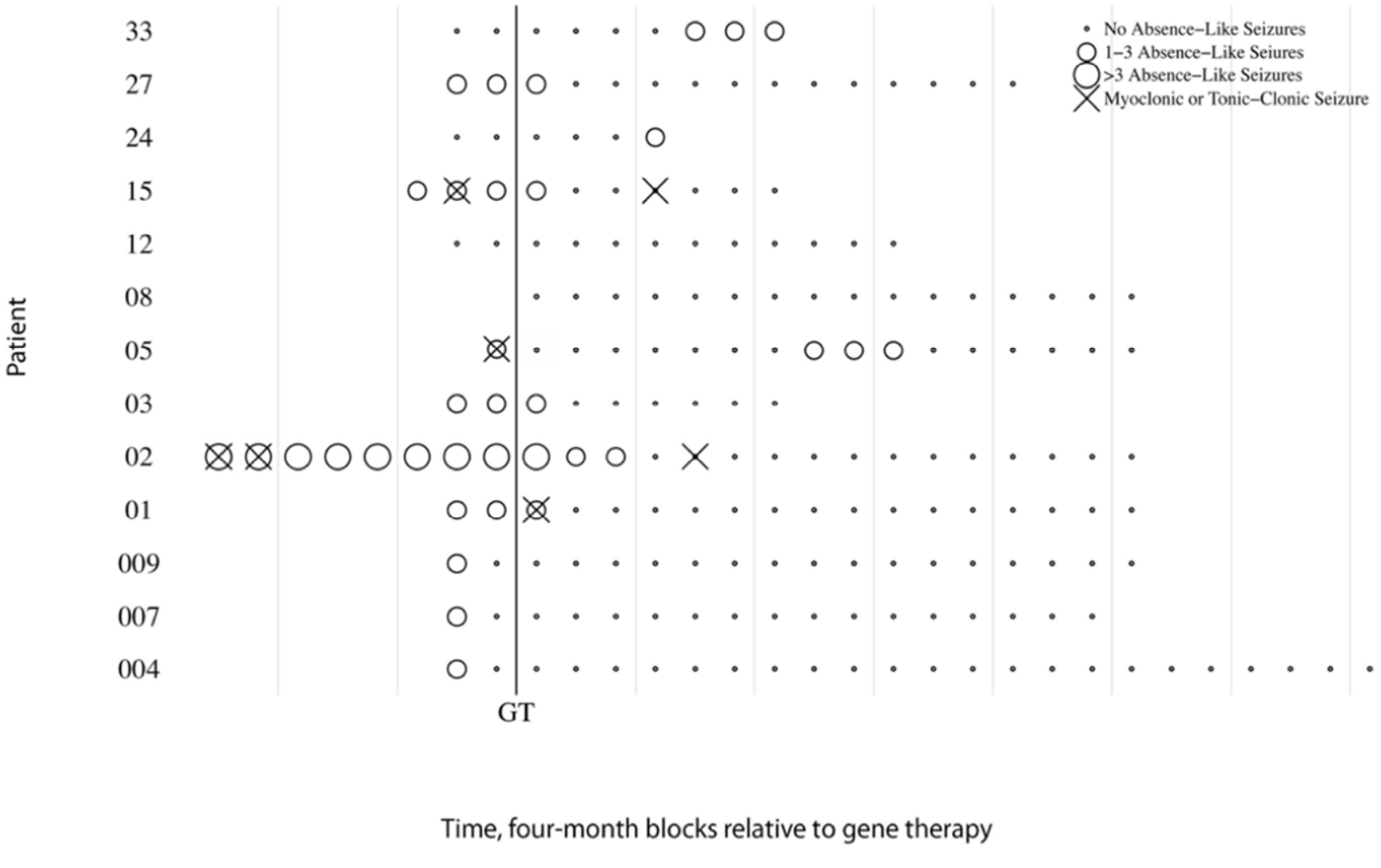

Fig. S9. Surgical procedure.

Intraoperative photo of 01-118-007, showing placement of six intracranial catheters during the gene therapy infusion procedure.